Electrical Double Layer at the Interface between Two Immiscible Electrolyte Solutions

ZDENĚK SAMEC

J. Heyrovský Institute of Physical Chemistry and Electrochemistry, Czechoslovak Academy of Sciences, U továren 254, 102 00 Prague, Czechoslovakia

Received March 23, 1987 (Revised Manuscript Received January 6, 1988)

Contents

Zdeněk Samec was born in 1947 and graduated from Charles University, Prague (1970). In 1973 he received his C.Sc. degree (equivalent to Ph.D.) and joined the J. Heyrovský Institute of Physical Chemistry and Electrochemistry, Czechoslovak Academy of Sciences, Prague. At present he is Head of the Group of Interfacial Charge Transfer and Deputy Head of the Electrochemistry Division. He was a postdoctoral fellow at the University of Michigan (1979) and visiting scientist at the University of Konstanz (1981) and Inorganic Chemistry Laboratory in Oxford (1982). His research interests include double-layer structure and charge-transfer kinetics across interface between two electrically conducting phases.

I. Scope

In recent years the electrochemical phenomena of liquid/liquid interfaces have attracted a great deal of interest due to the wide range of applications of these systems in chemistry and biology. In particular, the difference of electrical potentials between two contacting liquids and the interfacial charge transfer can play an important role in hydrometallurgy, phase-transfer catalysis, two-phase electrolysis, microemulsions for photochemical energy conversion, or the processes at liquid-membrane ion-selective electrodes and bilayer lipid membranes. Typically, such a liquid/liquid system consists of water (w) and an organic solvent (o) immiscible with it.

The variation of the electrical potential between two liquids, which underlies the mechanism and rate of the interfacial charge transfer as well as the stability and dynamics of these systems, is closely related to the distribution of the ionic and dipolar components across the liquid/liquid interface. In general, there is an excess electrical charge on one side of the interface, which in view of the electroneutrality condition has to be compensated by the excess opposite charge on the other side. Such a charge separation is usually referred to as the formation of the electrical double layer. Its existence at the interface between two immiscible electrolyte solutions (ITIES) had been envisaged by Risenfeld[1] as early as 1902, but the first quantitative treatment by Verwey and Niessen[2] came much later. According to Verwey,[3] the interfacial potential difference across the water/organic solvent interface can be divided into a surface potential caused by the orientation of dipoles and a double-layer potential related to ionic space charge. This idea has been revived by Gavach et al.[4] and developed further under the name of the modified Verwey–Niessen (MVN) model[5] (Figure 1).

This review deals with the equilibrium double layer at the ITIES. It is concerned primarily with the structure of the double layer, with its analysis in terms of thermodynamic and molecular models, and with its measurable surface tension and differential capacitance. Discussion is limited to polar solvent systems such as water/nitrobenzene or water/1,2-dichloroethane, the high dielectric permittivity of which ensures full or at least partial dissociation of electrolytes into ions. Most of the material presented here has been published since 1980. Although various aspects of electrochemical phenomena at liquid/liquid interfaces have been discussed,[6] a comprehensive and critical review-type treatment of the electrical double layer at the ITIES is lacking.

II. Thermodynamic Analysis

Gibbs Adsorption Equation

The thermodynamics of the electrical double layer at the ITIES was developed by several authors[4,7–10] for the interfacial models of Gibbs or Guggenheim.[11] The most general treatment was given by Kakiuchi and Senda.[10]

0009-2665/88/0788-0617$06.50/0

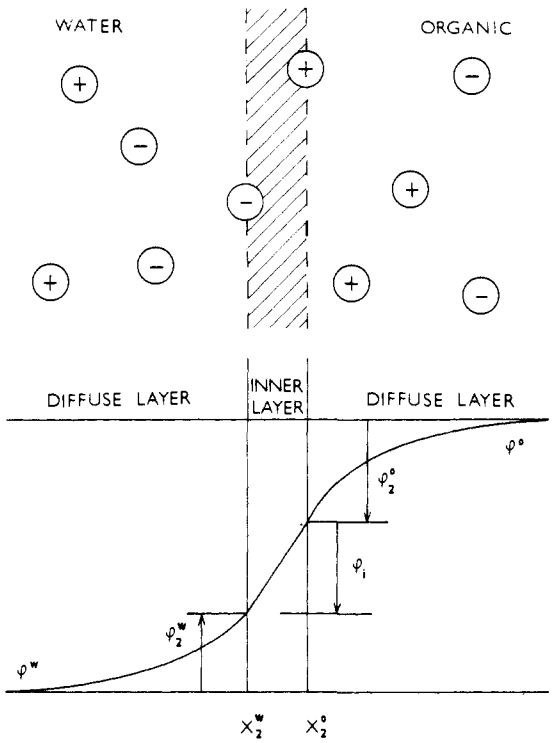

Figure 1. Modified Verwey-Niessen model of an ITIES and definition of potential differences involved. Full circles represent the point-charge ions, and x_2^w or x_2^o are positions of ions in planes of closest approach (outer Helmholtz planes) to the hypothetical plane of contact in the phase w or o, respectively. According to Gavach et al.[4]

At a constant temperature T and pressure p the change in the surface tension γ in the Gibbs model can be related to surface excess concentrations Γ^*_i of the species i through the Gibbs adsorption equation

$$-d\gamma(T,p=\text{const}) = \sum_i \Gamma^*_i \, d\tilde{\mu}_i \qquad (1)$$

where $\tilde{\mu}_i = \mu_i + z_i F\varphi$ is the electrochemical potential, μ_i is the chemical potential, z_i is the number of elementary charges (charge number) carried by the species i, F is the Faraday constant, and φ is the inner electrical potential of the phase (see list of symbols at the end of the paper). The surface excess concentration Γ^*_i is defined as

$$\Gamma^*_i = (n_i - n_i^w - n_i^o)/A \qquad (2)$$

where A is the interfacial area, n_i is the total number of moles of i in the whole system, n_i^σ is the number of moles of i in the interfacial region σ, and n_i^w or n_i^o is the number of moles of the same type that would be present in the homogeneous phase w or o, respectively, if that phase continued up to the fictitious plane of contact. The summation in eq 1 is carried out over all components in both phases. However, two variables can be eliminated by using the Gibbs–Duhem equation. Further reduction in the number of variables is possible upon considering the electrolyte dissociation and partition equilibria.

The equilibrium partition of an electrically neutral solute is characterized by the partition coefficient $K^{o,w}$

$$K^{o,w} = a_i^o/a_i^w \qquad (3)$$

where a_i^o and a_i^w are the activities of the solute i in the organic solvent and the aqueous phase, respectively.

The equilibrium partition of an ion gives rise to the electrical potential difference $\Delta_o^w\varphi = \varphi^w - \varphi^o$ between two phases (Nernst potential)[12,13]

$$\Delta_o^w\varphi = \Delta_o^w\varphi^o_i + (RT/z_iF) \ln (a^o_i/a_i^w) \qquad (4)$$

The standard potential difference $\Delta_o^w\varphi^o_i$ is defined as the equilibrium value of $\Delta_o^w\varphi$ at the unit ratio of ion activities a_i^o and a_i^w. It is closely related to the standard Gibbs energy of ion transfer from the aqueous phase to the organic solvent phase, $\Delta\bar{G}^o_{tr,i}$

$$\Delta_o^w\varphi^o_i = (\mu^{o,o} - \mu^{o,w})/z_iF = \Delta\bar{G}^o_{tr,i}/z_iF \qquad (5)$$

which is determined mainly by the resolvation energy.[14,15] Depending on the type of system, the interfacial potential difference $\Delta_o^w\varphi$ can be controlled in three different ways.

Nonpolarizable Interface

The simplest system is represented by the nonpolarizable interface, which is formed between two immiscible solvents w and o and in the presence of a single binary electrolyte RX. In each phase RX can dissociate into a cation R^+ and an anion X^- according to

$$RX = R^+ + X^- \qquad (6)$$

As a result of the partition equilibrium in the system

$$\underset{(w)}{R^+X^-} | \underset{(o)}{R^+X^-} \qquad (7)$$

where the perpendicular stroke represents the interface, the equilibrium potential difference $\Delta_o^w\varphi$ (distribution potential) will establish[12]

$$\Delta_o^w\varphi = (\Delta_o^w\varphi^o_R + \Delta_o^w\varphi^o_X)/2 + f(\gamma_i) \qquad (8)$$

where $f(\gamma_i) = (RT/2F) \ln (\gamma_+{}^w\gamma_-{}^o/\gamma_+{}^o\gamma_-{}^w)$ is the activity coefficients' term. Equation 8 implies that in this case $\Delta_o^w\varphi$ is independent of electrolyte concentration, which is actually the reason the interface is electrochemically nonpolarizable.

Gavach et al.[4] showed that for this system the Gibbs adsorption equation (eq 1) takes the simple form

$$-d\gamma(T,p=\text{const}) = \Gamma_{RX} \, d\mu_{RX} = 2RT\Gamma_{RX} d \ln a_\pm \qquad (9)$$

where μ_{RX} is the chemical potential of the electrolyte RX, $a_\pm$ is its mean activity, and Γ_{RX} is its relative surface excess

$$\Gamma_{RX} = \Gamma^*_{RX} - \Gamma^*_{H_2O}(n^w_{RX}/n^w_{H_2O}) - \Gamma^*_{org}(n^o_{RX}/n^o_{org}) \qquad (10)$$

The second and third terms on the right-hand side of eq 10 can usually be neglected, because $n^w_{RX}/n^w_{H_2O} \ll 1$ and $n^o_{RX}/n^o_{org} \ll 1$. Equation 9 then makes it possible to estimate the surface excess concentration of electrolyte Γ^*_{RX} from measurements of the surface tension at various mean activities of the electrolyte RX. We note that due to its partition equilibrium, $d\mu^w_{RX} = d\mu^o_{RX}$.

Girault and Schiffrin[8] used a similar approach but eliminated the other two quantities in eq 1 and obtained the expression for the relative surface excess of water

$$-d\gamma(T,p=\text{const}) = \Gamma_{H_2O} \, d\mu_{H_2O} \qquad (11)$$

where

$$\Gamma_{H_2O} = \Gamma^*_{H_2O} - \Gamma^*_{RX}(n^w_{H_2O}/n^w_{RX}) - \Gamma^*_{org}(n^o_{H_2O}/n^o_{org}) \qquad (12)$$

The complication connected with the use of eq 11 for the evaluation of the surface excess concentration of water $\Gamma^*_{H_2O}$ is evident. Whereas the third term on the right-hand side of eq 12 is rather small due to the inequality $n^o_{H_2O}/n^o_{org} \ll 1$, the second term can hardly be neglected, unless the surface excess concentration of the electrolyte $\Gamma^*_{RX} \approx 0$.

Ideally Polarizable Interface

The second type of system is the ideally polarizable ITIES. As shown by Koryta et al.[16] the system with two different electrolytes RX and SY in the phases w and o, respectively, can have the property of an ideally polarizable electrode. This can happen when the standard Gibbs energies of transfer for ions R^+ and X^- from w to o are large and positive and when the opposite is true for ions S^+ and Y^-. The potential difference $\Delta^w_o\varphi$ has the magnitude controlled by the excess electrical charge in the interfacial region, which can be supplied from an external source.

For the thermodynamic analysis of an ideally polarizable ITIES, it is convenient to consider the galvanic cell

$$M|M^+X^-|\underset{(w)}{R^+X^-}|\underset{(o)}{S^+Y^-}|\underset{(w')}{S^+Y^-}|M^+X^-|M' \qquad (13)$$

where M and M′ are two pieces of the same metal (e.g., silver between which the potential difference $E = \varphi^M - \varphi^{M'}$ is controlled or measured and $M|M^+X^-|R^+X^-$ and $M'|M^+X^-|S^+X^-$ are the reference electrodes reversible to an anion X^- (e.g., chloride) in the aqueous phases w and w′, respectively. The phases w′ and o contain a common cation S^+, the partition of which ensures that a constant potential difference across the w′/o interface is established.

For this case eq 1 can be written in the form of the Gibbs–Lippman (or electrocapillary) equation for the ideally polarizable mercury/electrolyte solution interface[9,10]

$$-d\gamma(T,p=\text{const}) = q(dE - d\mu_{SX}/F) + \Gamma_R\, d\mu_{RX} + \Gamma_Y\, d\mu_{SY} \qquad (14)$$

where the thermodynamic surface excess charge q is

$$q = -(\partial\gamma/\partial E)_{T,p,\mu} = F(\Gamma_R - \Gamma_X) \qquad (15)$$

and relative surface excesses Γ_i's are given by eq 10, in which the subscript i substitutes for RX. The electroneutrality condition reads

$$\Gamma_R + \Gamma_S = \Gamma_X + \Gamma_Y \qquad (16)$$

Since the ions R^+ and X^- or S^+ and Y^- are practically absence from phases o and w, respectively, their relative surface excess Γ_i's characterize the ion adsorption on the particular side s of the interface only (i.e., $\Gamma_i \approx \Gamma_i^s$) and the surface excess charge q acquires a simple physical meaning of the surface charge density on the side of the phase w, $q^w = F(\Gamma_R{}^w - \Gamma_X{}^w)$.

Girault and Schiffrin[9] analyzed the system as above but took into account the ion pairing in the bulk phase or at the interface, e.g.

$$R^+(w) + Y^-(o) \rightleftarrows R^+Y^-(o) \qquad (17)$$

In effect, q involves contributions from ion pairs R^+Y^- and S^+X^-

$$q = F(\Gamma_R - \Gamma_X + \Gamma_{RY} - \Gamma_{SX}) \qquad (18)$$

and the coefficients Γ_R and Γ_y in eq 14 have to be replaced by the sums $\Gamma_R + \Gamma_{RX} + \Gamma_{RY}$ and $\Gamma_Y + \Gamma_{SY} + \Gamma_{RY}$, which represent the total relative surface excesses of the cation R^+ or the anion Y^-, respectively.

Interface with Single Potential-Determining Ion

The third distinct type of system is represented by the ITIES with a single potential-determining ion. Under certain conditions the equilibrium potential difference across the ITIES is determined by the Nernst equation (eq 8). This may happen in the system described by the scheme 13 with a common cation $R^+ \equiv S^+$ or anion $X^- \equiv Y^-$, provided that the inequalities $\Delta^w_o\varphi^o_X \ll \Delta^w_o\varphi^o_R \ll \Delta^w_o\varphi^o_Y$ and $\Delta^w_o\varphi^o_S \ll \Delta^w_o\varphi^o_X \ll \Delta^w_o\varphi^o_R$, respectively, are fulfilled. As to the general thermodynamic analysis of the double layer, we refer again to the comprehensive treatment.[10] Particular cases were discussed later on in more detail.[17] The following example is illustrative. Consider the cell

$$M|M^+X^-|\underset{(w)}{S^+X^-}|\underset{(o)}{S^+Y^-}|M^+Y^-|M' \qquad (19)$$

with reference electrodes reversible to the anion X^- or Y^-. Equation 1 can be rewritten as follows:[17]

$$-d\gamma(T,p=\text{const}) = -F\Gamma_X\, dE + (\Gamma_X + \Gamma_Y)\, d\mu_{SY} \qquad (20)$$

or

$$-d\gamma(T,p=\text{const}) = F\Gamma_Y\, dE + (\Gamma_X + \Gamma_Y)\, d\mu_{SX} \qquad (21)$$

with $F\, dE = d\mu_{SX} + d\mu_{SY}$ and the electroneutrality condition $\Gamma_X + \Gamma_Y = \Gamma_S$. These equations show that the slope of the electrocapillary curve does not give the surface charge density, but only the relative surface excess of ionic components. However, it is important that this system can exhibit the electrocapillary behavior of an ideally polarizable ITIES as described by eq 14, on condition that another electrolyte RX is present in the phase w at a concentration much higher than that of SX and $\Delta^w_o\varphi^o_R \gg \Delta^w_o\varphi^o_S$.[7,17]

Relative surface excess Γ_i's or their linear combinations are experimentally accessible from the surface tension measurements. For an ideally polarizable ITIES, and under certain conditions also for the ITIES with a single potential-determining ion, there is another independent coefficient or state variable: the surface excess charge q. This quantity can be evaluated either by differentiation of the surface tension γ vs potential E plot or by integration of the differential capacitance C of the double layer

$$C = (\partial q/\partial E)_{T,p,\mu} = -(\partial^2\gamma/\partial E^2)_{T,p,\mu} \qquad (22)$$

which can be inferred from impedance measurements of the ITIES. The connection between the composition and the structure of the doubly layer can be established on the basis of a particular molecular model.

III. Models for Electrical Double Layer

Modified Verwey–Niessen Model

In the earliest treatment by Verwey and Niessen[2] the ITIES was represented by a diffuse double layer (i.e., one phase contains an excess of the positive space charge and the other phase an equal excess of the negative space charge), which was analyzed with the help of the theory of Gouy[18] and Chapman[19] (GC). By

analogy with Stern's modification[20] of the GC theory, Gavach et al.[4] introduced the concept of an ion-free layer of oriented solvent molecules, which separates the two space charge regions at the ITIES (see the MVN model in Figure 1).

In the MVN model the interfacial potential difference $\Delta_o^w\varphi$ splits into three contributions

$$\Delta_o^w\varphi = \varphi_i + \varphi_2^o - \varphi_2^w \quad (23)$$

where φ_i is the potential difference across the inner layer and φ_2^o and φ_2^w are the potential differences across the space charge regions in the phases o and w, respectively (Figure 1). When the Poisson–Boltzmann (PB) equation of Gouy and Chapman[18,19] is solved, two fundamental relationships are recovered between the surface excess charge q^s or the surface excess ion concentration $\Gamma_i^{*,s}$ on the side of the phase s and the corresponding potential difference φ_2^s.[21a,b] For the phase w

$$q^w = F(\Gamma_R^{*,w} - \Gamma_X^{*,w}) = -2A^w \sinh (F\varphi_2^w/2RT) \quad (24)$$

$$\Gamma_i^{*,w} = (A^w/F)[\exp(\mp F\varphi_2^w/2RT) - 1] \quad (25)$$

with

$$A^w = (2RT\epsilon^w\epsilon_0 c^{o,w})^{1/2} \quad (26)$$

where ϵ^w and ϵ_0 are the relative dielectric permittivity of water and the permittivity of vacuum, respectively, and $c^{o,w}$ is the bulk concentration of RX. The upper sign in eq 25 applies for the cation R^+, and the lower one for the anion X^-. Similar equations hold for the organic solvent phase.

On this basis, Gavach et al.[4] derived the following equation for the relative surface excess Γ_{RX} of a 1:1 electrolyte at the nonpolarizable ITIES

$$\Gamma_{RX} \approx \Gamma_{RX}^* = \Gamma_R^{*,w} + \Gamma_R^{*,o} = \Gamma_X^{*,w} + \Gamma_X^{*,o} = (A^w/F)\{[\exp(-F\varphi_2^w/2RT) - 1] + p^{1/2}[\exp(-F\varphi_2^o/2RT) - 1]\} \quad (27)$$

with $P = (\epsilon^o c^{o,o}/\epsilon^w c^{o,w})$. A straightforward implication of eq 27 is that Γ_{RX} is proportional to the square root of $c^{o,w}$, provided that $|\Delta_o^w\varphi - \varphi_i| = \text{const} \gg 2RT/F$.[4]

In the case of an ideally polarizable ITIES, the surface excess charge q^s and ion concentration $\Gamma_i^{*,s}$ are the quantities that are accessible to an independent evaluation from experiment. Therefore, the verification of their correlation implied by eq 24 and 25[22]

$$\Gamma_i^{*,s} = (A^s/F)(\pm y + (y^2 + 1)^{1/2} - 1) \quad (28)$$

with $y = q^s/2A^s$ represents a test of the GC theory. A decline from this correlation may indicate the failure of either assumptions involved (e.g., the assumption of the absence of specific ion adsorption) or the GC theory itself.

In the absence of the specific ion adsorption, the double-layer capacitance can be represented as a series combination of the inner-layer capacitance C_i and the diffuse double-layer capacitances $C_{2\text{-}o}$ and $C_{2\text{-}w}$[23]

$$C^{-1} = d\Delta_o^w\varphi/dq^w = C_i^{-1} + C_d^{-1} = C_i^{-1} + C_{2\text{-}w}^{-1} + C_{2\text{-}o}^{-1} \quad (29)$$

where $C_i = dq^w/d\varphi_i$ and

$$C_{2\text{-}s} = -dq^s/d\varphi_2^s = (FA^s/RT)\cosh(F\varphi_2^s/2RT) \quad (30)$$

Obviously, the capacitance of the diffuse double layer C_d has a minimum at $q^w = -q^o = 0$, the use of which can be made for the determination of the zero-charge potential difference from the capacitance data.[23,24] The minimum capacitance is proportional to the square root of the electrolyte bulk concentration.

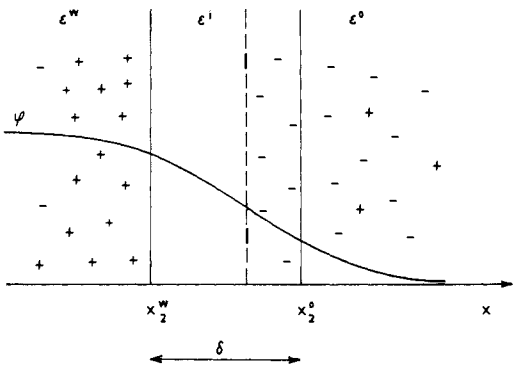

Figure 2. Model of an ITIES involving ion penetration into the inner layer. ϵ^w, ϵ^i, and ϵ^o are relative dielectric permittivities of the aqueous, inner layer, and organic solvent phase, respectively.[24]

Ion Interpenetration

Girault and Schiffrin[8] questioned the concept of an ion-free layer at the ITIES and suggested that a continuous change in composition from one phase to the other is a more realistic picture. However, their arguments in favor of the interfacial solvent mixing are not convincing. In fact, recent Monte Carlo experiments[25] have clearly indicated that the boundary formed between two immiscible liquids is sharp even in the presence of a model amphiphilic surfactant; i.e., the solvent density function shows an abrupt change at intermolecular distances.

On the other hand, there is obviously a nonzero probability of finding an ion in the inner-layer region.[5] Samec et al.[24] attempted to develop this idea by considering the MVN model, in which ions were allowed to penetrate into the inner layer over some distance (Figure 2), in analogy to the treatment of the electron spillover at the metal/electrolyte interface with the help of the nonlocal electrostatic approach.[26] When solvent is approximated by the dielectric continuum, the effect of ion penetration on the double-layer capacitance can be estimated by solving the linearized PB equation in all three regions of the MVN model. Then the inverse capacitance C^{-1} can be written as[24]

$$C^{-1} = C_i^{-1} + C_d^{-1} + \Delta \quad (31)$$

Capacitances C_i and C_d have the same meaning as in eq 29. In the linearized form they are expressed by

$$C_d^{-1} = (\epsilon_0\epsilon^w\kappa^w)^{-1} + (\epsilon_0\epsilon^o\kappa^o)^{-1} \quad (32)$$

$$C_i^{-1} = (\epsilon_0\epsilon^i)^{-1}\delta \quad (33)$$

where κ^{-1} is the Debye screening length

$$\kappa^{-1} = (F^2\sum_i z_i^2 c_i^o/\epsilon\epsilon_0 RT)^{-1/2} \quad (34)$$

δ is the inner-layer thickness and the superscript i refers to the inner layer. The parameter Δ, which accounts for the ion penetration, is given by

$$\Delta = (\epsilon^i\epsilon_0\kappa^i)^{-1}\left[\frac{(1 - h^2)\tanh(\kappa^i\delta)}{1 + h\tanh(\kappa^i/\delta)} - \kappa^i\delta\right] \quad (35)$$

where $h = (\epsilon^i\kappa^i/\epsilon^o\kappa^o)$. In the absence of the ion pene-

TABLE I. Reduced Potential Differences $\varphi^*_2 = F\varphi_2/RT$ in the Phase w ($\epsilon^w = 78.5$) and the Phase o ($\epsilon^o = 19.625$) for Point-Charge or Primitive Model Electrolytes[28]

φ^*_2(phase w)							φ^*_2(phase o)			
	IDL							IDL		
GC	without images	with images	ITIES	$c^{o,w}$, mol dm^{-3}	q, mC m^{-2}	$c^{o,o}$, mol dm^{-3}	ITIES	with images	without images	GC
1.40	1.38	1.43	1.41	0.01	8.87	0.005	2.38	2.39	2.94	3.02
4.08		3.99	3.89	0.01	44.35	0.005	3.71	3.82	4.29	6.14
0.47		0.50	0.48	0.10	8.87	0.05	1.03	1.05	1.19	1.25
2.03	1.94	2.01	1.95	0.10	44.35	0.05	2.24	2.27	2.76	3.84
1.21		0.95	0.93	1.0	75.57	0.50	0.85	0.97	1.21	2.71

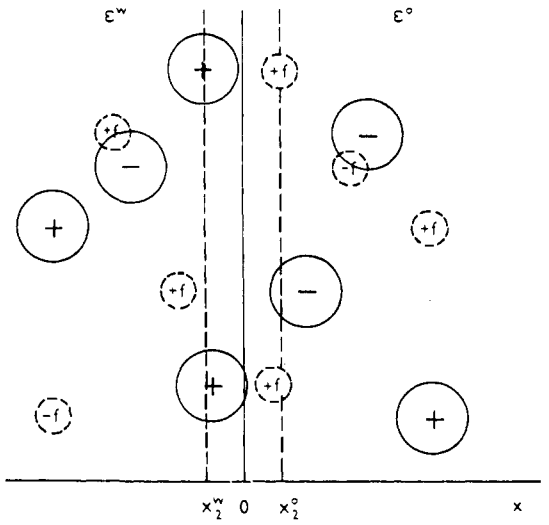

Figure 3. Primitive model of an ITIES. Full circles represent the finite-size ions with a charge number z, and smaller broken circles indicate fictitious image charges $z(\epsilon^w - \epsilon^o)/(\epsilon^w + \epsilon^o)$. According to Torrie and Valleau.[28]

tration the Debye screening length in the inner layer approaches infinity (i.e., $\kappa^i = 0$, $h = 0$, $\Delta = 0$), and eq 31 takes the form of eq 29. For $\kappa^i \neq 0$ the parameter Δ is negative and the inverse capacitance C^{-1} is reduced, which corresponds to a drop in the inner-layer potential difference φ_i.

Primitive Model of the ITIES

There are several reasons for which the PB equation may give an inadequate description of the electrical double layer.[27] Using the Monte Carlo (MC) technique, Torrie and Valleau[28] examined several features of the ITIES, which are not tractable by the GC theory, for the primitive model shown schematically in Figure 3. They considered in particular (a) ion–ion correlations within the space charge region, (b) ion–ion correlations between the two space charge regions, (c) interpenetration of the two space charge regions, and (d) image forces. Ion–ion correlations, the introduction of which makes it possible to account for the finite ion size, reduce the potential energy of the system and allow a thinner diffuse layer and smaller potential difference as compared with predictions of the GC theory. This feature was also examined with the help of other statistical-mechanical theories, such as those based on the modified Poisson–Boltzmann (MPB)[29] or hypernetted-chain (HNC)[30,31] equations; cf. Figure 4 for their comparison. Deviations from the GC theory increase with increasing z^2/ϵ;[26] e.g., the theoretical results for a 2:2 electrolyte in water ($\epsilon^w = 78.5$) are applicable to a 1:1 electrolyte in a solvent with dielectric permittivity of 19.625.

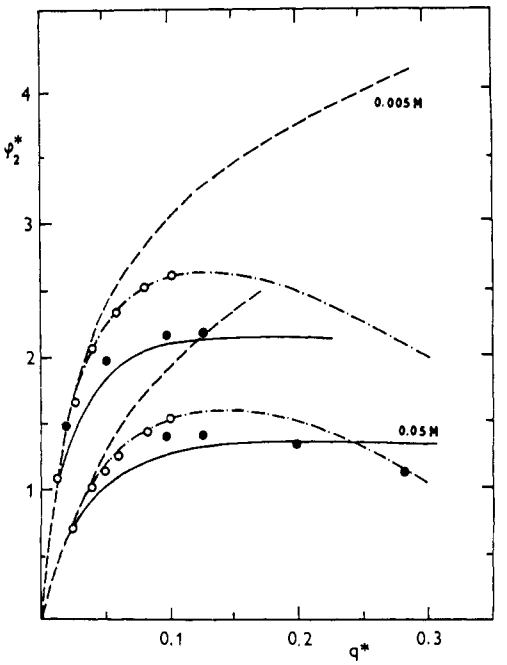

Figure 4. Dimensionless potential difference $\varphi^*_2 = F\varphi_2/RT$ across the space charge region for a 2:2 electrolyte (ion diameter 0.425 nm) in water ($\epsilon^w = 78.5$) vs surface charge density q^* ($q \approx 0.887q^*Cm^{-2}$) according to GC (– – –), HNC (–·–), noniterative HNC[32] (○), MPB (—), or MC (●) theories. Redrawn from ref 27.

Table I summarizes the reduced potential differences $\varphi^*_2 = F\varphi_2/RT$ across the space charge regions in the phase w ($\epsilon^w = 78.5$) and phase o ($\epsilon^o = 19.625$). They were calculated[28] with the help of the GC theory for the MVN model or with the help of the MC technique for the primitive model with independent double layers (IDL) in the presence or absence of image forces, or for the primitive model with image forces and between-layer ion correlation included (ITIES). It has been found that the GC theory describes the space charge region in the aqueous phase rather well, unless the electrolyte concentration is too large. On the other hand, discrepancies of the GC theory from theoretical predictions for more realistic models are considerable when the solvent dielectric permittivity is low. The between-layer ion correlations, by which the ITIES and IDL primitive models differ, seem to have little effect on the potential difference φ^*_2, so that the main source of these deviations is the within-layer ion correlations and image forces.

Specific Ion Adsorption

The molecular model, which accounts for the specific ion adsorption at the ITIES, was developed by Krylov et al.[33] The authors assumed that the concentration of

the electrolyte in each phase is high, so that the potential difference across the diffuse double layer can be neglected. They allowed the specifically adsorbed ions to approach a plane $x = x_1$ within the inner layer, which was composed of two solvent layers having dielectric permittivities ϵ^{iw} and ϵ^{io}. Provided that each ion occupies only a single adsorption site and the short-range interactions between ions can be treated as in the model of a two-dimensional van der Waals gas, the electrochemical potential $\tilde{\mu}_i^{ads}$ of the adsorbed ion is

$$\tilde{\mu}_i^{ads} = \mu^{o,ads} + RT \ln [\Gamma^*_i/(\Gamma^*_{im} - \Gamma^*_i)] - 2bRT(\Gamma^*_i\Gamma^*_{im}) + z_iF\int_0^1 \varphi_M(z_iF\xi)\, d\xi \quad (36)$$

where Γ^*_{im} is the maximum surface excess concentration of the ion, b is the attraction constant reflecting the nature of the short-range interactions, and φ_M is the local value of the electrical potential at the adsorption site, the so-called micropotential. The latter was calculated for the planar configuration of discrete charges and substituted into eq 36 to give after some rearrangements the equation of the Frumkin-type adsorption isotherm

$$Ba_i = [\theta_i/(1 - \theta_i)] \exp(-2b_{eff}\theta_i) \quad (37)$$

where B is a constant independent of the surface or bulk ion concentrations, $\theta_i = \Gamma^*_i\Gamma^*_{im}$ is the surface ion coverage, and the effective attraction constant b_{eff} is a function of geometric parameters and solvent dielectric permittivities.

IV. Electrochemical Polarization of the Interface

Most of the experimental results on the electrical double layer at the ITIES were obtained for the ideally polarizable interface, the thermodynamic state of which is controlled by supplying the electrical charge from the outside, i.e., by electrochemical polarization. In general, this can be accomplished by means of a four-electrode system[34,35] with two couples of potential-measuring (reference) and current-supplying (counter) electrodes. Under some conditions (e.g., low electrical current or large-area reference electrodes) three-[36] or two-electrode[37] systems can also be used, where one or two reference electrodes, respectively, comprise the function of both the reference and counter electrodes.

Electrochemical cells with a planar or spherical liquid/liquid boundary have been in common use. The former type is shown in Figure 5. Flatness of the boundary and the geometric configuration of the four electrodes are of critical importance for ensuring the homogeneous polarization of the liquid/liquid interface. For this reason, Senda et al.[37] made the inner space, which is in contact with the organic solvent, hydrophobic by treating it with dimethyldichlorosilane, while Buck et al.[39] inserted a piece of Teflon tubing into the cell. A spherical boundary is encountered in various assemblies with the hanging[36] (sitting)[40] or dropping[41-43] (ascending)[44] electrolyte electrode. A typical configuration is shown in Figure 6.

In these experiments the potential difference across the ITIES is controlled or measured usually with the help of Luggin probes or capillaries, the tips of which are typically about 1 mm from the boundary. When the

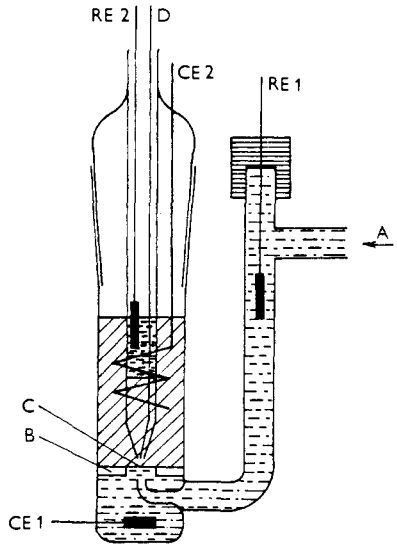

Figure 5. Scheme of the four-electrode cell with the planar liquid/liquid interface: (A) connection to a microsyringe for adjustment of the interface; (B) glass barrier with a round hole; (C) liquid/liquid interface; (D) insulated copper wire. CE1 and CE2 are platinum counter electrodes; RE1 and RE2 are silver/silver chloride reference electrodes. Reproduced with permission from ref 38. Copyright 1985 Elsevier Sequoia S.A.

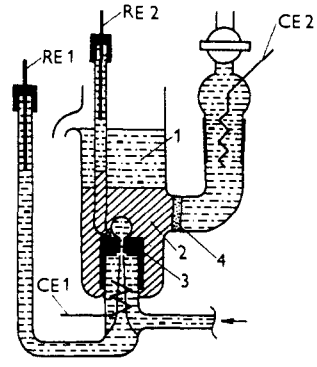

Figure 6. Scheme of the four-electrode cell with the spherical liquid/liquid interface (electrolyte drop electrode): (1) aqueous phase; (2) organic solvent phase; (3) PTFE cylinder with capillary; (4) sintered glass. According to Samec et al.[42]

electrical current flows through the ITIES, there is always a potential difference (ohmic potential drop) between the tip of a Luggin capillary and the point just outside the interfacial region on each side of the interface, by the sum of which the actual potential difference across the region differs from that measured or applied. Once measured, e.g., as the high-frequency limit of the interfacial impedance[23,45] or the potential step on the galvanostatic transient,[46] the ohmic potential drop can be accounted for by means of the positive feedback[35] or algebraic subtraction[46,47] under the potentiostatic or galvanostatic conditions, respectively.

In most of these experimental systems, the galvanic cell is represented by the scheme 13 (section II). The cell potential difference E can be written as

$$E = \Delta_o^w\varphi - \Delta_o^w\varphi^\circ_R - (RT/F) \ln (a_R{}^o/a_R{}^{w'}) - (RT/F) \ln (a_X{}^w/a_X{}^o) \quad (38)$$

The conversion of the potential E into the potential difference $\Delta_o^w\varphi$ is feasible, provided that the activities of ions R^+ and X^- and the standard potential difference $\Delta_o^w\varphi^\circ_R$ for the R^+ ion transfer are known. The activities of individual ions can be evaluated with the help of the

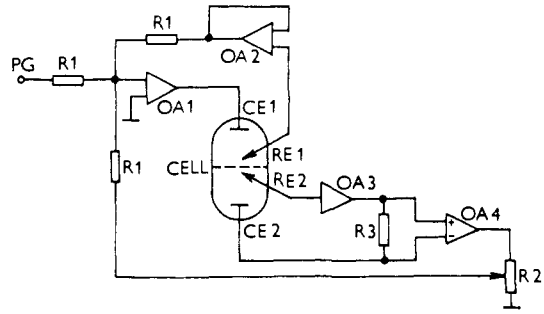

Figure 7. Block diagram of the electronic circuit of the four-electrode potentiostat with the positive feedback for the ohmic potential drop compensation. According to Samec et al.[5]

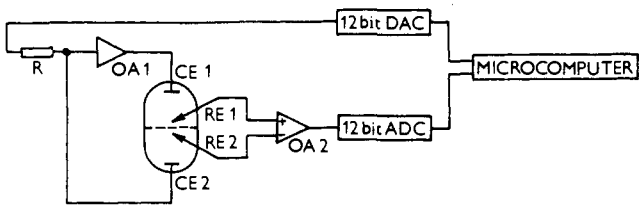

Figure 8. Block diagram of the electronic circuit for the galvanostatic pulse measurements. According to Samec et al.[5]

Debye–Hückel theory, but for low-permittivity solvents like 1,2-dichloroethane the ion association has to be taken into account.[45,48] Standard Gibbs transfer energies or standard potential differences for individual ions are not accessible to direct measurements, since they are always related to the corresponding quantity for another ion. Using an extrathermodynamic hypothesis, Rais[49] and Czapkiewicz and Czapkiewicz-Tutaj[50] evaluated standard Gibbs energies $\Delta\tilde{G}^{\circ}_{tr,i}$ of ion transfer from water to nitrobenzene and 1,2-dichloroethane, respectively, from extraction data. In the latter case, the comparison was made with the $\Delta\tilde{G}^{\circ}_{tr,i}$ values derived from solubility measurements.[51] Standard Gibbs energies of ion transfer between various solvents have been critically reviewed by Marcus.[52] A closer inspection of the voltammetric data reported in the literature indicated that the value $\Delta^{w}_{o}\varphi^{\circ}_{R} = -0.248$ V[15] for R^+ = tetrabutylammonium(+) (Bu_4N^+), on the basis of which the evaluations of the standard potential differences have been based most frequently, should be corrected by taking $\Delta^{w}_{o}\varphi^{\circ}_{R} = -0.275$ V.[5]

Potential difference across ITIES can be controlled by means of a potentiostat. A block schematic of the four-electrode potentiostat with the ohmic potential drop compensation based on the positive feedback[35] is shown in Figure 7. The potentiostat is driven by a voltage pulse generator (PG), and the current flowing through the cell is measured as the floating voltage drop across the measuring resistor R_3. A part of this voltage is fed back to the potentiostat for an automatic ohmic drop compensation. A two-electrode potentiostat was described by Senda et al.[37] In impedance measurements a small sinusoidal voltage signal, typically about 10 mV peak to peak, is superposed on the triangular voltage sweep[17,23,53] or applied at a constant potential (impedance method).[48] When the electrical current flowing through the ITIES is to be controlled, a galvanostat must be used, e.g., such as that shown schematically in Figure 8. Current perturbation is generated in the feedback loop of the operational amplifier OA1 by applying a voltage step or square voltage pulse[46] from a voltage pulse generator across the input resistor R. The introduction of the computer control made it possible to develop a fast-performance galvanostatic pulse technique for the measurement of the selected number of galvanostatic transients at different initial potentials over the whole potential range available.[38]

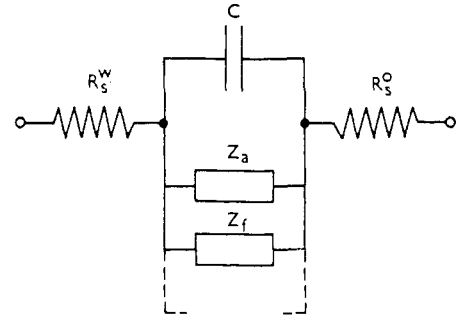

Figure 9. Electrical equivalent circuit for an ITIES. C is the capacitance of the double layer, Z_a is the adsorption impedance, Z_f is the faradaic impedance, and R_s^w or R_s^o is the solution resistance between tips of Luggin capillaries in the phase w or o, respectively.

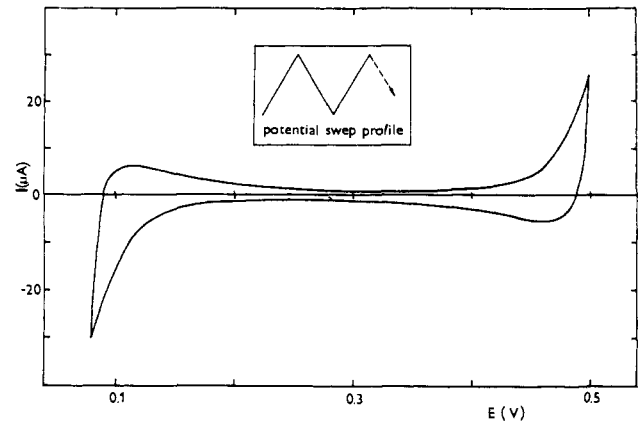

Figure 10. Cyclic voltammograms of the water/nitrobenzene interface at the sweep rate 0.1 V s^{-1}. Composition of the aqueous phase, 0.01 mol dm^{-3} NaBr; nitrobenzene phase, 0.01 mol dm^{-3} tetrabutylammonium tetraphenylborate; temperature, 298 K. Redrawn from ref 5.

Whereas the surface tension is accessible to a direct measurement, the differential capacitance C of the double layer at the ITIES has to be evaluated through a careful analysis of experimental impedance data. In general, an ITIES can be represented by the electrical equivalent circuit shown in Figure 9, which consists of the parallel combination of the double-layer capacitance C and the faradaic impedance Z_f with the solution resistance R_s between the tips of Luggin capillaries in series.[23] Specific adsorption of ions or neutral solutes can give rise to an additional (adsorption) impedance.[54,55] In order to minimize the faradic contribution, impedance measurements should be performed under the conditions in which the ion transfer is negligible and the system behaves as an ideally polarizable ITIES. Figure 10 shows the electrical current flowing through the water/nitrobenzene interface under the triangular voltage sweep excursion in the presence of the hydrophilic NaBr in water and the hydrophobic tetrabutylammonium tetraphenylborate (Bu_4NPh_4B) in nitrobenzene. In the potential range 0.13–0.45 V the current corresponds mainly to the double-layer charging and the system has the property required, while at more positive or more negative potentials, the interfacial

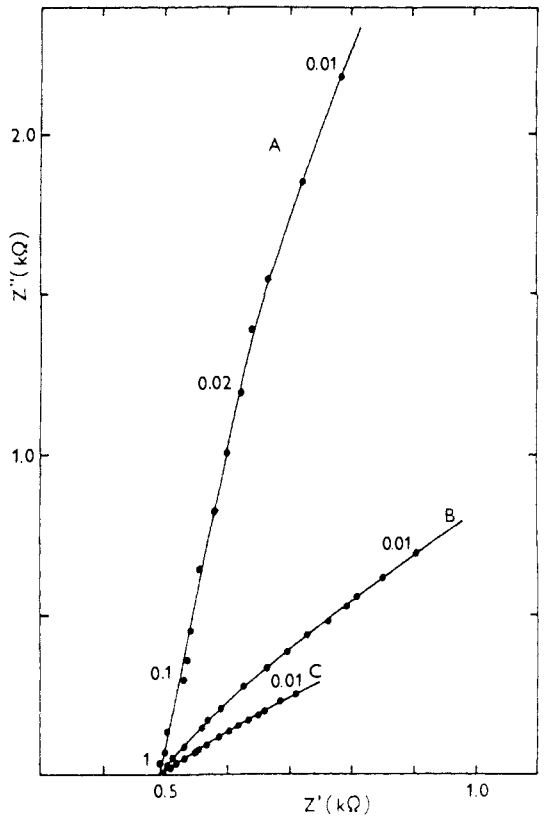

Figure 11. Impedance plot for the interface between 0.05 mol dm^{-3} LiCl in water and 0.05 mol dm^{-3} tetrabutylammonium tetraphenylborate in 1,2-dichloroethane at various potentials (vs Bu_4N^+): (A) 0.350 V; (B) 0.210 V; (C) 0.470 V. Numbers indicate the frequency in kilohertz. Reproduced with permission from ref 48. Copyright 1987 Elsevier Sequoia S.A.

transfer of ions present prevails.

The impedance of the ideally polarizable ITIES was measured by means of the alternating-current bridge[45] or phase-selective detection.[17,23,45,53-58] Results were usually presented in the form of the complex plane impedance. Its typical shape is illustrated in Figure 11. The high-frequency (>1 kHz) semicircle detected in some cases[55,57,58] was shown[58] to be due to artefactial capacitive coupling between the reference electrodes or was ascribed[57] to the geometric bulk-phase capacitance. Since the ion transfer is a rather fast process, the faradaic impedance Z_f can be replaced[22] by the Warburg impedance Z_W, corresponding to the diffusion-controlled process.[59] When the adsorption impedance Z_a can be neglected, the real Z' and the imaginary Z'' components of the complex impedance become[54]

$$Z' = |Z| \cos \beta = R_s + Z_C X[(X+1)^2 + 1]^{-1} \quad (39)$$

$$Z'' = |Z| \sin \beta = Z_C X(X+1)[(X+1)^2 + 1]^{-1} \quad (40)$$

where β is the phase shift between the applied and measured signal, $Z_C = (\omega C)^{-1}$, and $X = (Z_W/Z_C)(2^{1/2}) = 2fC\omega^{1/2}$, with f being the characteristic parameter of the faradaic process and w the angular frequency. In the analysis of impedance data, the solution resistance R_s is evaluated first as the high-frequency limit of Z; cf. Figure 11. The subsequent solution of eq 39 and 40 yields X and C. An alternative impedance method was tested by Samec and Mareček,[38,46] who used the galvanostatic pulse technique for the evaluation of the ohmic potential drop and capacitance of an ideally polarizable ITIES. When a current step $\delta I = I_0 = \text{const}$

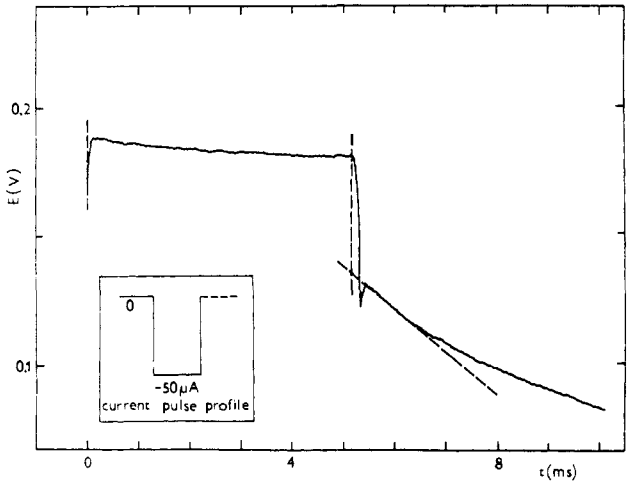

Figure 12. Galvanostatic transient at the water/nitrobenzene interface. Aqueous phase, 0.01 mol dm^{-3} NaBr; nitrobenzene phase, 0.01 mol dm^{-3} tetrabutylammonium tetraphenylborate; temperature, 298 K. Redrawn from ref 5.

is imposed on the interface, the charging current I_c decreases with time, while the faradaic current I_f increases. At very short times

$$\delta I = I_0 = I_c + I_f = C(dE/dt) + I_f \approx C(dE/dt)_0 \quad (41)$$

where dE/dt is the rate of the change of the potential difference across the interface. Under these conditions, the ohmic potential drop $\delta E_0 = I_0 R_s$ appears as a step on the galvanostatic transient at the beginning of the pulse ($t = t_0$) and the slope of this transient at $t > t_0$ is controlled only by the capacitance C (Figure 12).

V. Double-Layer Structure in the Absence of Specific Adsorption

Zero-Charge Potential Difference

Gavach et al.[7] and Buck et al.[60] used the drop-weight and maximum bubble pressure method, respectively, to measure the surface tension of the water/nitrobenzene interface in the presence of bromides of sodium (0.03 and 0.3 mol dm^{-3}) and tetraalkylammonium (1×10^{-6} to 2×10^{-3} mol dm^{-3}) ions in water and tetraalkylammonium tetraphenylborates (10^{-2} mol dm^{-3}) in nitrobenzene; i.e., tetraalkylammonium served as the potential-determining ion. The surface tension vs the potential difference $\Delta_o^w\varphi$ plots were constructed by varying the concentration of tetraalkylammonium bromide in water while holding constant the corresponding salt concentration in nitrobenzene. Comparison of the surface charge densities calculated with the help of the GC theory with those experimentally determined (eq 15) indicated that the potential difference is concentrated in the diffuse double layer and $\Delta_o^w\varphi_{pzc} = \varphi_i(q=0) = 1^7$ or 0 ± 5 mV.[60]

Kakiuchi and Senda[22,43] measured electrocapillary curves for the ideally polarizable interface between a nitrobenzene solution of Bu_4NPh_4B and an aqueous solution of LiCl at seven different concentrations of Bu_4NPh_4B (0.01–0.17 mol dm^{-3}) and LiCl (0.01–1.0 mol dm^{-3}) by the drop-weight/drop-time method using a dropping electrolyte electrode[43] at 25 °C. An example of the electrocapillary curve is shown in Figure 13. The zero-charge potential difference was practically independent of the concentration of both electrolytes and

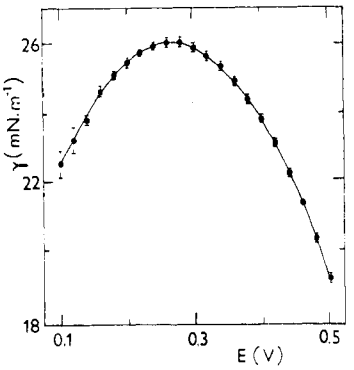

Figure 13. Surface tension γ vs potential E for the interface between 0.1 mol dm^{-3} LiCl in water and 0.1 mol dm^{-3} tetrabutylammonium tetraphenylborate in nitrobenzene at 298 K. Vertical bars indicate the standard devaition for triplicate measurements. Reproduced with permission from ref 43. Copyright 1983 The Chemical Society of Japan.

was estimated as $\Delta_o^w\varphi_{pzc} \approx 0.020$ V[22] on the basis of the standard potential difference $\Delta_o^w\varphi^\circ_R = -0.248$ V for the reference Bu_4N^+ cation. If the corrected value $\Delta_o^w\varphi^\circ_R = -0.275$ V[5] is used instead, the zero-charge potential difference becomes $\Delta_o^w\varphi_{pzc}$; −0.007 V, which is obviously very close to zero. Girault and Schiffrin[9] reported surface tension data for the ideally polarizable interface between 0.01 mol dm^{-3} KCl in water and 0.001 mol dm^{-3} Bu_4NPh_4B in 1,2-dichloroethane, obtained by a pendant-drop video-image digitizing technique.[40] Results were found to be in good agreement with the doubly integrated capacitance obtained from galavanostatic pulse experiments. An independent measurement of the potential of zero charge by the streaming-jet electrode technique[61] gave a value identical with the potential of the electrocapillary maximum. On the basis of the standard potential difference $\Delta_o^w\varphi^\circ_R = -0.225$ V[51] for the Bu_4N^+ ion transfer, the zero-charge potential difference was estimated from these data as equal to 8 ± 10 mV,[62] by taking into account the association of Bu_4NPh_4B in 1,2-dichloroethane ($K_a = 1.715 \times 10^3$ dm^3 mol^{-1}).[51] Samec et al.[48] measured the surface tension for the interface between 0.01 mol dm^{-3} LiCl in water and 0.01 mol dm^{-3} Bu_4NPh_4B in 1,2-dichloroethane and evaluated $\Delta_o^w\varphi_{pzc}$ = 10 mV on the same grounds.

Samec et al.[23] suggested that the minimum of capacitance (Figure 14) should correspond to the zero-charge potential difference. This is indicated by eq 29: when $C_i^{-1} \ll C_d^{-1}$, the capacitance $C \approx C_d$ passes through a minimum at $q = 0$ ($\varphi_2^w = \varphi_2^\circ = 0$). The values of the potential difference $\Delta_o^w\varphi^\circ$ corresponding to the capacitance minimum in various systems are summarized in Table II. A small positive shift of $\Delta_o^w\varphi^\circ$ with increasing electrolyte concentration, which is most pronounced for the aqueous LiCl solutions, was ascribed to the variation of the inner-layer capacitance C_i with the surface charge density.[24] On this basis the conclusion was made that for all the systems studied the zero-charge potential difference $\Delta_o^w\varphi_{pzc} \approx 0$ mV.[5,23,24,56] The capacitance evaluated from impedance measurements for water/1,2-dichloroethane shows a single minimum at a potential difference close to that for the electrocapillary maximum (Figure 15). The zero-charge potential difference was then estimated as 10–20 mV.[48] Other values reported, namely, $\Delta_o^w\varphi_{pzc}$ = 1[54] and 35[45] mV, are based on a limited number of experimental data and are therefore less accurate.

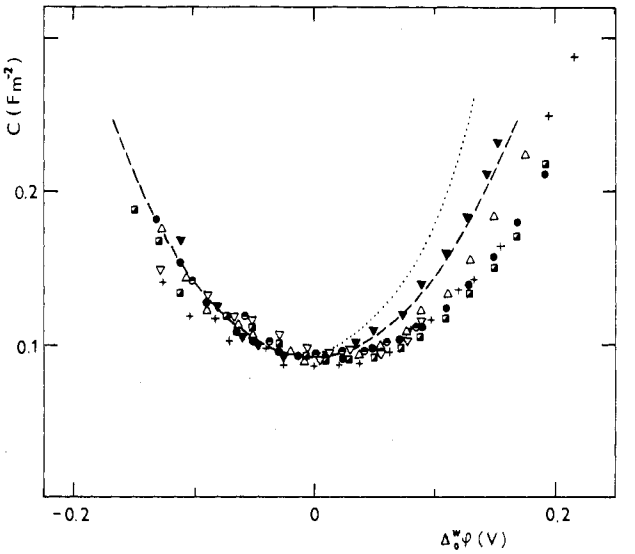

Figure 14. Differential capacitance C of the double layer at the interface between 0.01 mol dm^{-3} LiCl (●), NaCl (◪), KCl (▽), RbCl (⊖), NaBr (△), and LiBr (+) or 0.005 mol dm^{-3} $MgCl_2$ (▼) in water and 0.01 mol dm^{-3} tetrabutylammonium tetraphenylborate in nitrobenzene at 298 K. Lines: capacitance of the diffuse double layer calculated assuming that φ_i = const = 0 for a 1:1 electrolyte in nitrobenzene and a 1:1 (dashed) or 1:2 (dotted) electrolyte in water. Reproduced from ref 64.

TABLE II. Potential Difference $\Delta_o^w\varphi^\circ$ at Minimum Capacitance of the Water/Nitrobenzene Interface in the Presence of Tetrabutylammonium Tetraphenylborate in Nitrobenzene and LiCl (I), NaBr (II), $MgSO_4$ (III), and $MgCl_2$ (IV) in Water at 298 K[24]

$c^{o,o}$,[a] mol dm^{-3}	$\Delta_o^w\varphi^\circ$, mV			
	I[b]	II	III	IV[c]
0.005		11		−15
0.010	18 (15)	5	3	−15
0.020	(25)	4	−8	−9
0.050	24 (29)	0	15	−5
0.100	50 (45)	11	16	

[a] For NaBr and LiCl $c^{o,w} = c^{o,o}$; for $MgSO_4$ and $MgCl_2$ $c^{o,w} = c^{o,o}/2$. [b] Data in parentheses are from ref 23. [c] Unpublished except for $c^{o,o}$ = 0.01 mol dm^{-3}.[56]

In summary, the zero-charge potential difference $\Delta_o^w\varphi_{pzc} = 0 \pm 10$ mV was found for both the water/nitrobenzene and water/1,2-dichloroethane systems, irrespective of the type and concentration of electrolytes present. This points to the absence of the specific adsorption of ions and neutral solutes at the interface. It is noteworthy that the scatter of the capacitance[24,48] or the surface tension[43] data is often greater than the variation of the capacitance or the surface tension around the minimum or maximum, respectively. Though the reproduciblity of the estimation of $\Delta_o^w\varphi_{pzc}$ from both measurements is very good, the actual value seems to depend somewhat on the statistical method used in data processing.

Structure of the Diffuse Double Layer

By using the drop-weight technique, Gavach et al.[4] measured the surface tension of the nonpolarizable water/nitrobenzene interface in the presence of various tetraalkylammonium (alkyl = ethyl, propyl, butyl, or pentyl) halides. With increasing salt concentration, the relative surface excess Γ_{RX} of the salt RX (eq 9) increased, as shown in Figure 16. The behavior of the tetraethyl-, tetrapropyl-, and tetrabutylammonium

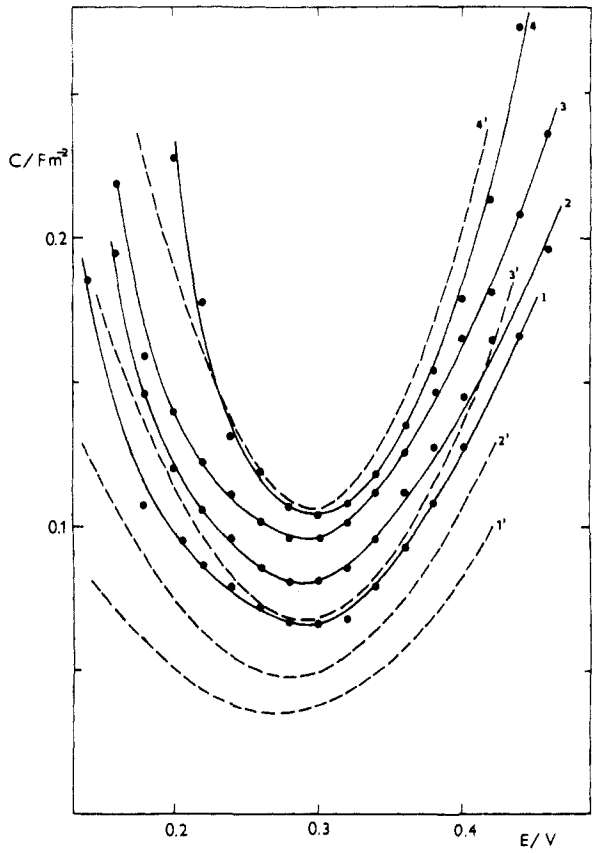

Figure 15. Differential capacitance C of the double layer at the water/1,2-dichloroethane interface for various concentrations (in mmol dm^{-3}) in LiCl in water and tetrabutylammonium tetraphenylborate in 1,2-dichloroethane: 5 (1, 1'); 10 (2, 2'); 20 (3, 3'); 50 (4, 4') (temperature, 298 K). Dashed lines: capacitance of the diffuse double layer calculated with the GC theory assuming that φ_i = const = 0. Reproduced with permission from ref 48. Copyright 1987 Elsevier Sequoia S.A.

bromides conforms with the GC theory in that Γ_{RX} is proportional to the square root of the aqueous electrolyte concentration, as predicted by eq 27. The change in slope of the plot in Figure 16 is due to the parameter P, which is controlled by the salt partition coefficient (eq 3), and due to the potential differences φ_2^w or φ_2^o across the space charge regions of the aqueous or organic solvent phase, respectively. In fact, when $\Delta_o^w\varphi$ is large and negative as for these electrolytes, $F\varphi_2^w/RT \gg 1$, $F\varphi_2^o/RT \ll 1$, and $\Gamma_{RX} \approx (A^w/RT)P^{1/4}$ exp$[-F(\Delta_o^w\varphi - \varphi_i)/4RT]$. Boguslavsky et al.[63] also studied this type of system and observed qualitatively similar behavior over the broad concentration range up to the limit given by the solubility of the tetraalkylammonium salt used. However, their interpretation is based solely on the Krylov model,[33] eq 36 and 37, which may not be applicable at low electrolyte concentration.

By means of eq 14, Kakiuchi and Senda[22] evaluated the surface excess charge q and relative surface excess Γ_i (cf. eq 14) of Li^+, Cl^-, Bu_4N^+, and Ph_4B^- ions at the ideally polarizable water/nitrobenzene interface. Figure 17 shows Γ_{Li} and Γ_{Cl} as functions of q^w. Theoretical plots were constructed with the help of eq 10, where the subscript i substitutes for RX. Γ^*_i was calculated from eq 28. The last term in eq 10 was neglected, because $n_i^o/n_{org}^o \to 0$. With the assumption that the structure of water on the surface is the same as in the bulk, $\Gamma^*_{H_2O}$ was estimated as the bulk concentration per unit area $N_A^{-1}(N_A/V_m)^{2/3} = 1.73 \times 10^{-9}$ mol cm^{-2}, where N_A is

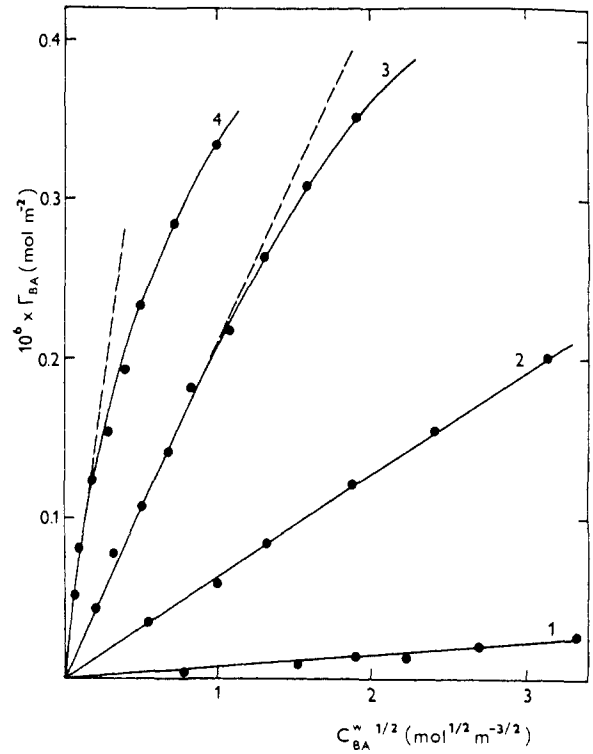

Figure 16. Relative surface excess Γ_{BA} at the water/nitrobenzene interface vs the square root of the electrolyte concentration in the aqueous phase c_{BA}^w for (1) tetraethylammonium bromide, (2) tetrapropylammonium bromide, (3) tetrabutylammonium bromide, and (4) tetrapentylammonium bromide. According to Gavach et al.[4]

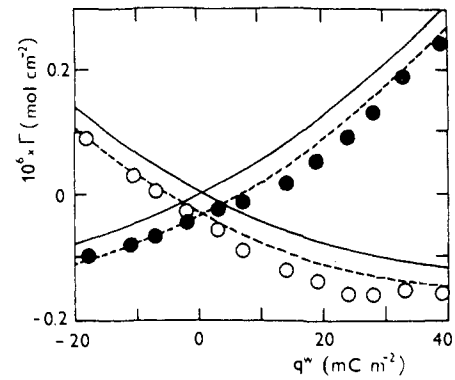

Figure 17. Relative surface excess of Li^+ (●) and Cl^- (○) ions in the aqueous phase as a function of the surface charge density in the aqueous phase for 0.1 mol dm^{-3} LiCl. Solid lines, theoretical curves based on the GC theory; dashed lines, after correction for exclusion of Li^+ and Cl^- ions from the inner layer. Reproduced with permission from ref 22. Copyright 1983 The Chemical Society of Japan.

Avogradro's number and V_m is the molar volume of water. However, arguments[21b] supporting this estimation of $\Gamma^*_{H_2O}$ are somewhat obscure. In an alternative approach,[21c] which follows a straightforward procedure based on eq 2, the surface excess concentration of water was estimated as the difference between the surface and bulk concentrations per unit area. Then for the surface water having the structure of the bulk solvent as assumed above, $\Gamma^*_{H_2O} = 0$. For a hexagonal array of surface water molecules of radius $r_{H_2O} = 0.138$ nm, $\Gamma^*_{H_2O} = (2(3^{1/2})N_A r_{H_2O}^2)^{-1} - N_A^{-1}(N_A/V_m)^{2/3} = 0.79 \times 10^{-9}$ mol cm^{-2}, which is about half the value above. In order to reach agreement with experimental data, a layer of water molecules on the surface somewhat thicker than

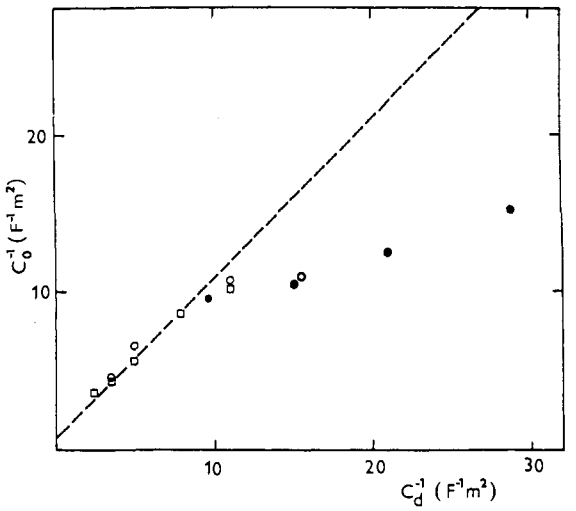

Figure 18. Inverse capacitance C^{-1} at the zero surface charge vs the inverse capacitance of the diffuse double layer C_d^{-1} calculated with the GC theory for LiCl in water and tetrabutylammonium tetraphenylborate in 1,2-dichloroethane (●), LiCl in water and tetrabutylammonium tetraphenylborate in nitrobenzene (○), and NaBr in water and tetrabutylammonium tetraphenylborate in nitrobenzene (□). Dashed line corresponds to the equation $C_0^{-1} = 0.8 + C_d^{-1}$. Reproduced with permission from ref 48. Copyright 1987 Elsevier Sequoia S.A.

the monolayer would have to be considered. In any case, the plots in Figure 17 as well as the values of the Jesin–Markov coefficients $(\partial E/\partial \mu_{RX})_{q,\mu_{SY}}$ and $(\partial E/\partial \mu_{SY})_{q,\mu_{RX}}$ indicated that the adsorption of all ions occurs primarily in diffuse parts of the double layer on both sides of the interface. A similar analysis of surface tension data for the ideally polarizable water/1,2-dichloroethane interface was not undertaken, in part because of the presumed unclear physical meaning of the thermodynamic excess charge q in this case; cf. eq 18.[9]

Capacitance data were reported for ideally polarizable interfaces between the nitrobenzene solution of Bu_4NPh_4B and the aqueous solution of LiCl,[17,23,24,58,64] NaCl,[64] NaBr,[5,24,64] KCl,[64] RbCl,[64] $MgSO_4$,[24] or $MgCl_2$,[56] between the nitrobenzene solution of Ph_4AsPh_4B and the aqueous solution of LiCl[24,56,64] or NaCl,[53] and between the 1,2-dichloroethane solution of Bu_4NPh_4B and the aqueous solution of LiCl.[45,48,54] Experimental capacitances were compared with the capacitance C_d of the diffuse double layer calculated by means of the GC theory; cf. dashed lines in Figures 14 and 15. At least for the water/nitrobenzene system and medium concentrations, the capacitance C is described well by eq 29 and 30, which is in agreement with the picture emerging from the surface tension measurements.

However, the GC theory tends to underestimate the capacitance of the space charge region at low electrolyte concentrations.[5,24] This tendency is even more pronounced for the water/1,2-dichloroethane interface.[48] Figure 18 shows the experimental inverse capacitance C^{-1} at the zero surface charge plotted against the inverse GC capacitance of the diffuse double layer C_d^{-1}. For the water/nitrobenzene interface this correlation satisfies eq 29 with $C_i \approx 1$ F m^{-2} at higher electrolyte concentrations, whereas there is a drop from the expected straight line at low electrolyte concentrations, which would correspond to the physical unacceptable value of the inner-layer capacitance ($C_i < 0$). For the water/1,2-dichloroethane interface such a drop is apparent over the whole range of concentrations studied. These discrepancies were suggested[5,24,48] to be due to the inadequate description of the space charge region by the GC theory, as explained in section III.

TABLE III. Values of Ion-Free Layer Thickness d at Water/Organic Solvent Interfaces[8]

	d^a			
	LiCl	NaCl	KCl	$MgSO_4$
nitrobenzene	0.4	0.7	0.4	3.0
1,2-dichloroethane	0.4	0.9	0.6	
n-heptane	0.9		1.0	
air–solution	0.9	1.0	1.0	2.2

[a] Expressed as monolayers of water, assuming that $d = 1$ corresponds to $\Gamma_{H_2O} = 1.72 \times 10^{-9}$ mol cm^2.

Structure of the Inner Layer

The first attempt to analyze the structure of the inner layer at the ITIES was made by Girault and Schiffrin,[8] who measured the surface tension of the nonpolarizable ITIES in the presence of various inorganic salts. From eq 11 they evaluated the relative surface excess of water at the water/nitrobenzene, water/1,2-dichloroethane, and water/*n*-heptane interfaces and estimated the thickness of the ion-free layer (Table III). The latter was dependent on the polarity of the organic phase: *n*-heptane gave thicknesses similar to those observed for the air/solution interface, but the polar solvents gave values less than unity. The authors suggested that both mixed solvation and interfacial mixing are responsible for this effect, and the conclusion was made that this is the reason for the apparent absence of an ion-free inner layer at the ITIES, as indicated by low values of the inner-layer potential difference[17,22] or high values of the inner-layer capacitance.[5,24] Here use was obviously made of the assumption that the second and third terms on the right-hand side of eq 12 can be neglected. Actually, because the standard Gibbs transfer energies of inorganic cations and anions involved are nearly equal, the corresponding standard potential differences compensate for each other, so that the distribution potential (eq 8) is close to zero, and probably $\Gamma^*_{RX} \approx 0$.

High values of the inner-layer capacitance $C_i \approx 0.8$–1.0 F m^{-2} at $q = 0$[5,17,24] can hardly correspond to the inner layer consisting of two adjacent solvent monolayers.[5,8,24,62] Assuming a random orientation of monomeric water ($\epsilon^w \approx 20$) and nitrobenzene ($\epsilon^o \approx 35$) molecules, the capacitance of such a bilayer can be estimated as $C_i = (2r_{H_2O}/\epsilon^w\epsilon_0 + 2r_{org}/\epsilon^o\epsilon_0)^{-1} \approx 0.28$ F m^{-2} for molecular radii of water $r_{H_2O} = 0.155$ nm and nitrobenzene $r_{org} = 0.278$ nm,[15] which were estimated from molar volumes. Therefore, the penetration of ions from the nitrobenzene phase into the inner layer (Figure 2) was examined with eq 31–35 for $\delta = 1.6$ nm, $\epsilon^i = 25$, and $\kappa^i = (\epsilon^o/\epsilon^i)^{1/2}\kappa^o$, which corresponds to an extension of the Boltzmann ion distribution from the region with the dielectric permittivity ϵ^o into the region with the permittivity ϵ^i. At higher electrolyte concentrations the theory reproduces experimental data well, but it fails to follow the drop in the inverse capacitance at low concentrations (Figure 18). When, instead, the Debye screening length was estimated from $f\kappa^i = (\epsilon^o/\epsilon^i)^{1/2}\kappa^o$, with f being the adjustable parameter, the theoretical fit for the experimental capacitance of the interface

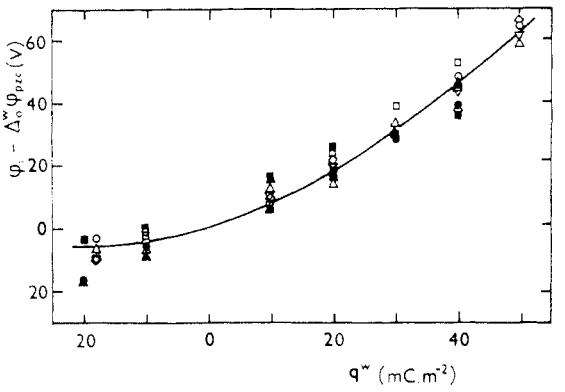

Figure 19. Potential difference φ_i (relative to zero-charge potential difference $\Delta_o^w\varphi_{pzc}$) vs the surface charge density q^w in the aqueous phase for the interface between LiCl in water and tetrabutylammonium tetraphenylborate in nitrobenzene. LiCl concentration is 0.05 (□), 0.1 (△), 0.2 (◇), 0.5 (▽), and 1.0 (○) mol dm^{-3} when organic salt concentration is 0.1 mol dm^{-3}, and the organic salt concentration is 0.05 (■), 0.1 (●), and 0.17 (▲) mol dm^{-3} when the LiCl concentration is 0.1 mol dm^{-3}. Reproduced with permission from ref 22. Copyright 1983 The Chemical Society of Japan.

between aqueous NaBr and nitrobenzene Bu_4NPh_4B solutions was reached for f = 0.41, 0.72, 1.00, 1.05, 1.25, or 1.50 at electrolyte concentrations 0.005, 0.01, 0.02, 0.05, 0.1, or 0.2 mol dm^{-3}, respectively. Qualitatively, this corresponds to a slower variation of the screening length in the inner layer than in the space charge regions.

Figure 19 shows the variation of the inner-layer potential difference φ_i at the water/nitrobenzene interface with the surface charge density q^w, as inferred from the surface tension measurements by means of the GC theory.[17,22] As one can expect for the MVN model in the absence of the specific ion adsorption, the value of φ_i at a constant q^w is independent of electrolyte concentrations. We note that the inner-layer potential difference is close to zero at low electrolyte concentrations, for which $|q^w| < 10$ mC m^{-2}. It is gratifying that an independent evaluation of φ_i from capacitance data yields similar results (Figure 20).[17,64] Samec et al.[24] took into account the finite size of ions and evaluated the potential difference $\varphi_2^o - \varphi_2^w$ across the diffuse double layer by the noniterative procedure,[32] which makes use of the HNC equation.[30,31] The substitution of $\varphi_2^o - \varphi_2^w$ into eq 23 gave the value of the inner-layer potential difference φ_i corresponding to the surface charge density q, which was found by integration of the experimental capacitance vs the potential plot. For all the water/nitrobenzene systems studied, this procedure led to somewhat greater estimates of φ_i; cf. Figure 20.

A similar analysis of the capacitance data for the water/1,2-dichloroethane system has not been possible yet, though there has been some evidence indicating that the inner-layer potential difference φ_i is small.[45,48,54] Samec et al.[48] applied the weak-coupling equations[65] to the primitive model of an ITIES (Figure 3) and compared the effect of image forces for the water/nitrobenzene and water/1,2-dichloroethane interfaces. They concluded that the image forces together with the within-layer ion correlations are more likely to be responsible for a virtual rise of the experimental capacitance of the water/1,2-dichloroethane interface over the GC value (Figures 15 and 18) than the interfacial ion pairing.[9] In fact, from a physical point of view it would not be clear why ion pairs such as $Li^+Ph_4B^-$ or $Bu_4N^+Cl^-$ should concentrate just at the interface, in particular when they are absent from the bulk of each phase.

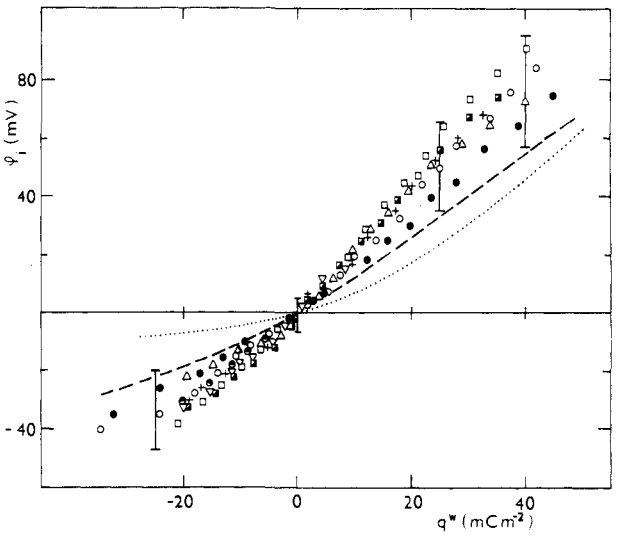

Figure 20. Potential difference φ_i at the water/nitrobenzene interface as a function of the surface charge density q^w evaluated from the experimental data by using the noniterative HNC results for the diffuse double layer at 298 K. Nitrobenzene phase: 0.05 mol dm^{-3} tetrabutylammonium tetraphenylborate (●, ◪, △, +) or tetraphenylarsonium dicarbonylcobaltate (□, ○); aqueous phase: LiCl (●, ○, □), NaCl (◪), NaBr (△), and LiBr (+). Dahses line: average evaluated from the same experimental data by using the GC theory; dotted line: average from Figure 19.

VI. Specific Adsorption of Ions and Neutral Solutes

A remarkable drop in the surface tension of the water/1,2-dichloroethane interface was observed in the presence of natural phospholipids (phosphatidylcholine, phosphatidylethanolamine)[66] or triazine dyes (Cibabron Blue F36A, Procion Blue MX-R) modified by a long-chain carbon residue.[67] The effect of phosphatidylcholine is illustrated in Figure 21. Two potential regions can be distinguished: at potentials negative with respect to a critical value (region A), a very small change of surface tension with potential is observed, while a rapid increase of surface tension with potential is seen at more positive potentials (region B). It was suggested that region A corresponds to the adsorption of the phospholipid as a zwitterion, whereas in region B the surface reorientation of the phosphatidylcholine layer occurs accompanied by neutralization of its phosphate group and the electrocapillary curve corresponds to the behavior of a cationic surfactant. Triazine dyes show a similar, though more involved, electrocapillary behavior with an intermediate region characterized by a sudden change in the surface tension, which corresponds probably to a surface phase transition resulting in a stacked structure of the polar heads and in a close packing of the hydrophobic carbon chains.[67] On the other hand, due to neutralization of its primary amine group, phosphatidylethanolamine can start to behave as an anionic surfactant at more negative potentials, also causing an increase in the surface tension.[66] The relationship between the acid–base properties of adsorbed molecules and the stability domains of phospholipids or triazine dye layers was discussed.[66,67]

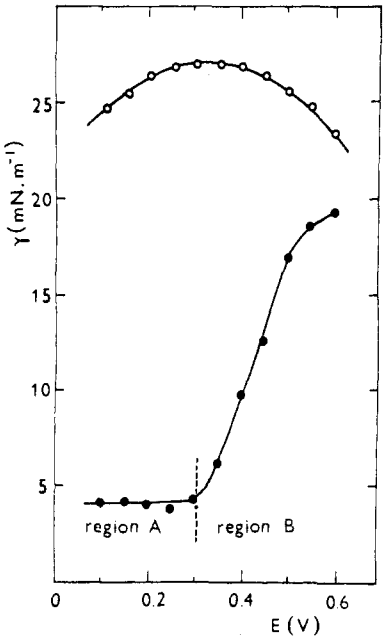

Figure 21. Potential dependence of the surface tension of the water/1,2-dichloroethane interface for a solution containing 0.01 mol dm^{-3} KCl in water (pH 5) and 0.001 mol dm^{-3} tetrabutylammonium tetraphenylborate in 1,2-dichloroethane (○); idem after the addition of phosphatidylcholine to a concentration of 25×10^{-6} mol dm^{-3} (●) (temperature, 298 K). Redrawn from ref 66.

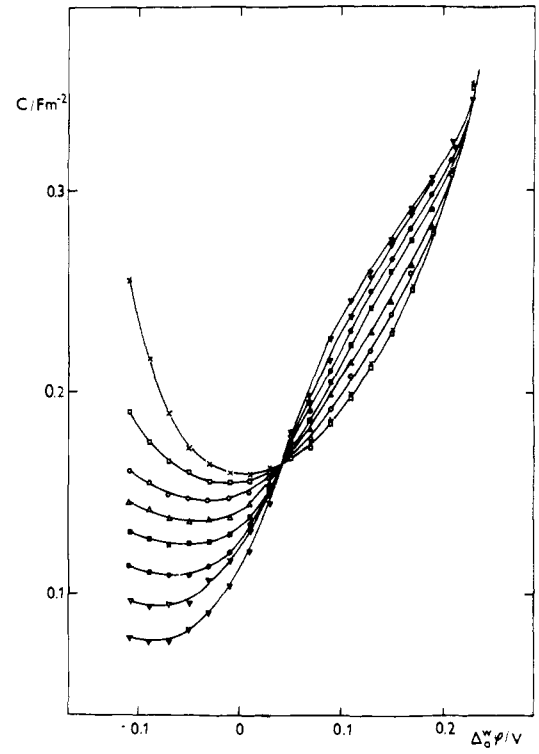

Figure 22. Differential capacitance C of the double layer at the interface between 0.05 mol dm^{-3} LiCl in water and 0.05 mol dm^{-3} tetrabutylammonium tetraphenylborate in nitrobenzene in the presence of 1,2-dipalmitoyl-*sn*-glycero-3-phosphatidylcholine at concentrations 0 (×), 0.15 (□), 0.4 (○), 0.8 (△), 1.2 (■), 3.0 (●), 6.0 (▽), and 20 (▼) μmol dm^{-3} in nitrobenzene (temperature, 298 K). Reproduced with permission from ref 70. Copyright 1988 Elsevier Sequoia S.A.

The effect of synthetic phosphatidylcholines on the structure of the ITIES is rather different. In particular, no phase transition in the adsorbed layer was observed to occur. Senda et al.[68] and Samec et al.[69,70] used the impedance technique for measurements of adsorption of 1,2-dilauroyl- (DLPC), 1,2-dimyristoyl- (DMPC), and 1,2-dipalmitoyl-*sn*-glycero-3-phosphatidylcholine (DPPC) at the water/nitrobenzene interface. A strong and potential-dependent adsorption was indicated by a drop in the double-layer capacitance at potentials negative to the potential of zero charge (Figure 22). Senda et al.[68] evaluated the surface coverage θ of a phospholipid by using the relation $C = (1 - \theta)C^\circ + \theta C^{sat}$, where C° is the capacitance C in the absence of adsorbate and C^{sat} is the saturated value of C. The surface coverage fitted in the Langmuir isotherm, indicating small lateral interactions between the adsorbed molecules.[68] However, Frumkin's original treatment of adsorption of neutral substances at an electrode, which underlies this evaluation, is equivalent to a model of the double layer consisting of two capacitors in parallel, one containing solvent molecules and the other containing organic molecules. As reference is obviously made to the ion-free layer (the inner layer), the surface coverage θ of an adsorbate at the ITIES should be calculated instead from the inner-layer capacitance C_i by the same relation as above.[70] The surface coverage evaluated in this way from impedance data fits the Frumkin adsorption isotherm (eq 37) with the adsorption Gibbs energy decreasing in the sequence DLPC > DMPC > DPPC from −35.7 to −37.9 kJ mol^{-1} and the attraction constant equal to −0.4.[70] This points to a strong adsorption of all three phosphatidylcholines with repulsive yet weak lateral interactions in the adsorbed layer. The observed increase in the inner-layer potential difference as well as the positive shift of the zero-charge potential difference is probably connected with the preferential orientation of the adsorbed phosphatidylcholine molecules at the interface with their polar heads or hydrocarbon chains directed toward the aqueous or organic solvent phase, respectively.[70]

Senda et al.[71,72] have studied the adsorption of hexadecyltrimethylammonium ($HexMe_3N^+$) and cetyltrimethylammonium ($CetMe_3N^+$) ions at the ideally polarizable water/nitrobenzene interface by means of the surface tension[71,72] and impedance[72] measurements. The adsorption of both cationic surfactants was also found to be strongly dependent on the interfacial potential difference $\Delta_o^w\varphi$. $HexMe_3N^+$ exhibited no specific adsorption in the potential range where the aqueous phase is positive, whereas a strong adsorption occurred in the potential range where the inner electrical potential φ^w in the aqueous phase was negative with respect to that in nitrobenzene (Figure 23).[71] The polar head groups of both $HexMe_3N^+$ and $CetMe_3N^+$ protrude into the aqueous side of the interface and cause a significant change in the structure of the diffuse double layer.[71,72] As a result, the potential difference φ_2° across the nitrobenzene space charge region is inverted from a negative to a positive value. The degree of binding of the aqueous counterion (Cl^-) to the adsorbed monolayer of $CetMe_3N^+$ ion was estimated.[72] The importance of these effects in the physical chemistry of emulsions and artificial or biological membranes is evident.[71]

VII. Concluding Remarks

Classical electrochemical methods have been successfully adapted for the study of the ITIES. Knowl-

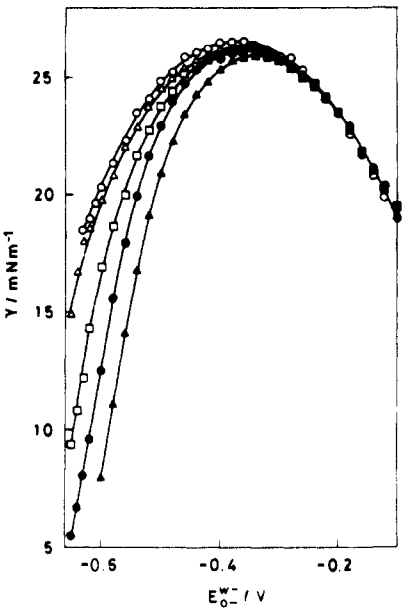

Figure 23. Electrocapillary curves for the interface between 0.05 mol dm^{-3} LiCl in water and (0.1 − x) mol dm^{-3} tetrapentylammonium tetraphenylborate and x mol dm^{-3} hexadecyltrimethylammonium tetraphenylborate in nitrobenzene at 298 K: x = 0 (○), 0.005 (△), 0.02 (□), 0.05 (●), and 0.1 (▲). Reproduced with permission of ref 71. Copyright 1987 The Chemical Society of Japan.

edge gained by their application has advanced complex physicochemical understanding of various electrochemical phenomena at liquid/liquid interfaces.

The difference of the inner electrical potentials $\Delta_o^w\varphi$ between water (w) and an organic solvent (o) can be controled in three different ways: by means of the equilibrium partition of a salt (nonpolarizable ITIES), equilibrium ion-transfer reaction (ITIES with a single potential-determining ion), or electrical charge supplied from the outside (ideally polarizable ITIES). In general, such a potential difference is the driving force of a charge-transfer reaction and must be considered as one of the key factors controlling selectivities and rates of the mass transfer across the ITIES in systems of practical interest.

The modified Verwey–Niessen model,[3,4] in which an inner layer of solvent molecules separates two space charge regions (diffuse double layer), describes the structure of an ITIES well, provided that ions are allowed to penetrate into the inner layer over some distance.[5,24] It has been also proposed that the inner layer is a thin mixed-solvent layer of about one or two molecules of solvent diameter thickness, which ions from both sides can penetrate partially.[62] In any case, the liquid/liquid boundary is sharp; i.e., a drop or rise in density of one or the other solvent, respectively, occurs at molecular distances.

Apart from the detailed structure of the inner layer, ion and solvent distribution functions can hardly be regarded as monotonic functions of distance when inspected on a molecular scale. In fact, theoretical calculations for the ion and dipole mixture model,[73] which is more realistic than a primitive model electrolyte,[27] show that both functions have an oscillatory character, indicating the inevitable stratification connected with the finite size of the ion and solvent molecules. The ion distribution in the diffuse double layer is governed primarily by electrostatic interactions. Since these depend on the ratio (z^2/ϵ), in the sequence water < nitrobenzene < 1,2-dichloroethane, the effects become more pronounced of the ion association, ion size, and image forces. Specifically adsorbed ionic and neutral surfactant molecules modify the structure of the inner layer, change the magnitude and eventually the sign of the inner-layer potential difference, and induce variations in the ion distribution in both space charge regions. Factors responsible for phase transitions in the adsorbed layer at the ITIES have not been fully understood, but research along this line is progressing.

The quantitative description of the ion and potential distribution is of fundamental importance for elucidation of the charge-transfer kinetics across the ITIES. Two basic effects have to be expected. First, the existence of a solvent inner layer with its specific structure as compared with the solution bulk can introduce an additional barrier to be overcome for an ion crossing the interface. Second, the charge-transfer rate is dependent on actual concentrations of reactants, i.e., on their distribution in the interfacial region. Kinetic analysis, which accounts for the ion distribution across the ITIES, was carried out for the transfer of (a) tetraalkylammonium,[37,47,74] picrate,[75,76] and Cs^+ [35,77] ions, (b) alkaline earth metal cations facilitated by poly(ether diamides)[78] and Na^+ ion facilitated by dibenzo-18-crown-6,[79] and (c) electron transfer between ferrocene and hexacyanoferrate(III),[77] all across the water/nitrobenzene interface. The properties of the kinetic barrier in the inner layer were examined by means of a stochastic approach.[80]

VIII. List of Symbols and Acronyms

a	activity
A	interfacial area
b	attraction constant; b_{eff}, effective attraction constant
c	concentration; $c°$, bulk concentration
C	differential capacitance of the double layer; C_i, capacitance of the inner layer; C_d, capacitance of the diffuse double layer; C_{2-s}, capacitance of the space charge region in phase s
d	dimensionless thickness of the inner layer (number of monolayers)
E	cell potential difference
F	Faraday's constant
$\Delta\tilde{G}°_{tr,i}$	standard Gibbs energy of ion transfer from water to organic solvent
I	electrical current
$K^{o,w}$	partition coefficient for interface between phases w and o
n	number of moles
N_A	Avogadro's number
o	organic solvent phase
p	pressure
r	radius
R	gas constant
R_s	electrical resistance of electrolyte solutions
q	surface charge density
s	phase s
t	time
T	absolute temperature
V_m	molar volume
x	coordinate perpendicular to the interface

w	aqueous phase
z	charge number
Z	impedance; Z', real component; Z'', imaginary component; Z_a, adsorption impedance; Z_W, Warburg impedance; Z_C, capacitive impedance
β	phase shift
γ	surface tension, activity coefficient
Γ	relative surface excess
Γ^*	surface excess concentration; Γ^*_m, maximum surface excess concentration
δ	thickness of the inner layer
ϵ	relative dielectric permittivity; ϵ_0, permittivity of vacuum
θ	surface coverage
κ	inverse Debye screening length of the space charge region
$\tilde{\mu}$	electrochemical potential; μ, chemical potential; μ°, standard chemical potential
φ	inner electrical potential; $\Delta_o^w\varphi = \varphi^w - \varphi^o$, difference of inner electrical potentials between phases w and o; $\Delta_o^w\varphi_{pzc}$, zero-charge potential difference; $\Delta_o^w\varphi^\circ$, standard potential difference; φ_2, potential difference across the space charge region; φ_i, potential difference across the inner layer
ω	angular frequency
GC	Gouy–Chapman
HNC	hypernetted chain
IDL	independent double layers
ITIES	interface between two immiscible electrolyte solutions
MC	Monte Carlo
MPB	modified Poisson–Boltzman
MVN	modified Verwey–Niessen
PB	Poisson–Boltzmann

IX. References

(1) Risenfeld, E. H. *Ann. Phys.* **1902**, *8*, 616–624.
(2) Verwey, E. J. W.; Niessen, K. F. *Philos. Mag.* **1939**, *28*, 435–446.
(3) Verwey, E. J. W. *Colloid Science*; Kruyt, H. R., Ed.; Elsevier: Amsterdam, 1952; Vol. 1, p 137.
(4) Gavach, C.; Seta, P.; d'Epenoux, B. *J. Electroanal. Chem. Interfacial Electrochem.* **1977**, *83*, 225–235.
(5) Samec, Z.; Mareček, V.; Homolka, D. *Faraday Discuss. Chem. Soc.* **1984**, *77*, 197–208.
(6) (a) Vanýsek, P. "Electrochemistry on Liquid/Liquid Interfaces". *Lect. Notes Chem.* **1985**, *39*, 3–109. (b) Kazarinov, V. E., Ed. *The Interface Structure and Electrochemical Processes at the Boundary between Two Immiscible Liquids*; Springer-Verlag: Berlin, Heidelberg, 1987.
(7) Gros, M.; Gromb, S.; Gavach, C. *J. Electroanal. Chem. Interfacial Electrochem.* **1978**, *89*, 29–36.
(8) Girault, H. H.; Schiffrin, D. J. *J. Electroanal. Chem. Interfacial Electrochem.* **1983**, *150*, 43–49.
(9) Girault, H. H. J.; Schiffrin, D. J. *J. Electroanal. Chem. Interfacial Electrochem.* **1984**, *170*, 127–141.
(10) Kakiuchi, T.; Senda, M. *Bull. Chem. Soc. Jpn.* **1983**, *56*, 2912–2918.
(11) Guggenheim, E. A. *Thermodynamics*; North-Holland: Amsterdam, 1959.
(12) Karpfen, F. M.; Randles, J. E. B. *Trans. Faraday Soc.* **1953**, *498*, 823–831.
(13) Hung, Le Q. *J. Electroanal. Chem. Interfacial Electrochem.* **1980**, *115*, 159–174.
(14) Kornyshev, A. A.; Volkov, A. G. *J. Electroanal. Chem. Interfacial Electrochem.* **1984**, *180*, 363–381.
(15) Abraham, M. H.; Liszi, J. *J. Inorg. Nucl. Chem.* **1981**, *43*, 143–151.
(16) Koryta, J.; Vanýsek, P.; Březina, M. *J. Electroanal. Chem. Interfacial Electrochem.* **1977**, *75*, 211–228.
(17) Senda, M.; Kakiuchi, T.; Osakai, T.; Kakutani, T. *The Interface Structure and Electrochemical Processes at the Boundary between Two Immiscible Liquids*; Kazarinov, V. E., Ed.; Springer-Verlag: Berlin, Heidelberg, 1987; pp 107–121.
(18) Gouy, G. *C. R. Acad. Sci.* **1910**, *149*, 654–657.
(19) Chapman, D. L. *Philos. Mag.* **1913**, *25*, 475–481.
(20) Stern, O. *Z. Elektrochem.* **1924**, *30*, 508–516.
(21) (a) Parson, R. *Modern Aspects of Electrochemistry*; Bockris, J. O'oM., Conway, B. E., Eds.; Butterworths: London, 1954; pp 103–179. (b) Mohilner, D. M. *Electroanalytical Chemistry*; Bard, A. J., Ed.; Marcel Dekker: New York, 1966; Vol. 1, pp 241–409. (c) Habib, M. A.; Bockris, J. O'M. *Comprehensive Treatise of Electrochemistry*; Bockris, J. O'M., Conway, B. E., Yeager, E., Eds.; Plenum: New York, London, 1980; Vol. 1, pp 135–219.
(22) Kakiuchi, T.; Senda, M. *Bull. Chem. Soc. Jpn.* **1983**, *56*, 1753–1760.
(23) Samec, Z.; Mareček, V.; Homolka, D. *J. Electroanal. Chem. Interfacial Elctrochem.* **1981**, *126*, 121–129.
(24) Samec, Z.; Mareček, V.; Homolka, D. *J. Electroanal. Chem. Interfacial Electrochem.* **1985**, *187*, 31–51.
(25) Yurtsever, E.; Karaasian, H. *Ber. Bunsen-Ges. Phys. Chem.* **1987**, *91*, 600–603.
(26) Kornyshev, A. A.; Schmickler, W.; Vorotyntsev, M. A. *Phys. Rev. B* **1982**, *25*, 5244–5256.
(27) Carnie, S. L.; Torrie, G. M. **1984**, *56*, 141–253.
(28) Torrie, G. M.; Valleau, J. P. *J. Electroanal. Chem. Interfacial Electrochem.* **1986**, *206*, 69–79.
(29) Outhwaite, C. W.; Bhuiyan, L. B.; Levine, S. *J. Chem. Soc., Faraday Trans. 2* **1980**, *76*, 1388–1408.
(30) Carnie, S. L.; Chan, D. Y. C.; Mitchell, D. J.; Ninham, B. W. *J. Chem. Phys.* **1981**, *74*, 1472–1478.
(31) Lozada-Cassou, M.; Saavedra-Barreza, R.; Henderson, D. *J. Chem. Phys.* **1982**, *77*, 5150–5156.
(32) Henderson, D.; Blum, L. *J. Electroanal. Chem. Interfacial Electrochem.* **1980**, *111*, 217–222.
(33) Krylov, V. S.; Myamlin, V. A.; Boguslavsky, L. I.; Manvelyan, M. A. *Elektrokhimiya* **1977**, *13*, 834–840; *Soviet. Electrochem. (Engl. Transl.)* **1977**, *13*, 707–712.
(34) Gavach, C.; Henry, F. *J. Electroanal. Chem. Interfacial Electrochem.* **1974**, *54*, 361–370.
(35) Samec, Z.; Mareček, V.; Weber, J. *J. Electroanal. Chem. Interfacial Electrochem.* **1979**, *100*, 841–852.
(36) Mareček, V.; Samec, Z. *Anal. Lett.* **1981**, *14*, 1241–1253.
(37) Osakai, T.; Kakutani, T.; Senda, M. *Bull. Chem. Soc. Jpn.* **1984**, *57*, 370–376.
(38) Mareček, V.; Samec, Z. *J. Electroanal. Chem. Interfacial Electrochem.* **1985**, *185*, 263–271.
(39) Melroy, O. R.; Bronner, W. E.; Buck, R. P. *J. Electrochem. Soc.* **1983**, *130*, 373–380.
(40) Girault, H. H.; Schiffrin, D. J.; Smith, B. D. V. *J. Electroanal. Chem. Interfacial Electrochem.* **1982**, *137*, 207–217.
(41) Koryta, J.; Vanýsek, P.; Březina, M. *J. Electroanal. Chem. Interfacial Electrochem.* **1976**, *67*, 263–266.
(42) Samec, Z.; Mareček, V.; Weber, J.; Homolka, D. *J. Electroanal. Chem. Interfacial Electrochem.* **1979**, *99*, 385–389.
(43) Kakiuchi, T.; Senda, M. *Bull. Chem. Soc. Jpn.* **1983**, *56*, 1322–1326.
(44) Yoshida, Z.; Freiser, H. *J. Electroanal. Chem. Interfacial Electrochem.* **1984**, *162*, 307–319.
(45) Geblewicz, G.; Figaszewski, Z.; Koczorowski, Z. *J. Electroanal. Chem. Interfacial Electrochem.* **1984**, *177*, 1–12.
(46) Mareček, V.; Samec, Z. *J. Electroanal. Chem. Interfacial Electrochem.* **1983**, *149*, 185–192.
(47) Samec, Z.; Mareček, V. *J. Electroanal. Chem. Interfacial Electrochem.* **1986**, *200*, 17–33.
(48) Samec, Z.; Mareček, V.; Holub, K.; Račinský, S.; Hájková, P. *J. Electroanal. Chem. Interfacial Electrochem.* **1987**, *225*, 65–78.
(49) Rais, J. *Collect. Czech. Chem. Commun.* **1971**, *36*, 3253–3262.
(50) Czapkiewicz, J.; Czapkiewicz-Tutaj, B. *J. Chem. Soc., Faraday Trans. 1* **1980**, *76*, 1663–1668.
(51) Abraham, M. H.; Danil de Namor, A. F. *J. Chem. Soc., Faraday Trans. 1* **1976**, *72*, 955–962.
(52) Marcus, Y. *Pure Appl. Chem.* **1983**, *55*, 977–1021.
(53) Reid, J. D.; Vanýsek, P.; Buck, R. P. *J. Electroanal. Chem. Interfacial Electrochem.* **1984**, *161*, 1–15.
(54) Hájková, P.; Homolka, D.; Mareček, V.; Samec, Z. *J. Electroanal. Chem. Interfacial Electrochem.* **1983**, *151*, 277–282.
(55) Berlouis, L. A.; Chatman, J.; Girault, H. H. J.; Schiffrin, D. J. *Extended Abstracts of the Electrochemical Society Spring Meeting*, San Francisco, May 8–13, 1983; p 935.
(56) Homolka, D.; Hájková, P.; Mareček, V.; Samec, Z. *J. Electroanal. Chem. Interfacial Electrochem.* **1983**, *159*, 233–238.
(57) Reid, J. D.; Vanýsek, P.; Buck, R. P. *J. Electroanal. Chem. Interfacial Electrochem.* **1984**, *170*, 109–125.
(58) Silva, F.; Moura, C. *J. Electroanal. Chem. Interfacial Electrochem.* **1984**, *177*, 317–323.
(59) Sluyters-Rehbach, M.; Sluyters, J. H. *Comprehensive Treatise of Electrochemistry*; Yeager, E., Sarangapani, S., Eds.; Plenum: New York, London, 1984; pp 177–292.

(60) Reid, J. D.; Melroy, O. R.; Buck, R. P. *J. Electroanal. Chem. Interfacial Electrochem.* **1983**, *147*, 71–82.
(61) Girault, H. H. J.; Schiffrin, D. J. *J. Electroanal. Chem. Interfacial Electrochem.* **1984**, *161*, 415–417.
(62) Girault, H. H. J.; Schiffrin, D. J. *J. Electroanal. Chem. Interfacial Electrochem.* **1985**, *195*, 213–227.
(63) Boguslavsky, L. I.; Frumkin, A. N.; Gugeshashvili, M. I. *Elektrokhimiya* **1976**, *12*, 856–860; *Sov. Electrochem. (Engl. Transl.)* **1976**, *12*, 799–802.
(64) Wandlowski, T.; Mareček, V.; Samec, Z. *J. Electroanal. Chem. Interfacial Electrochem.*, submitted.
(65) Reference 27, pp 169–175.
(66) Girault, H. H. J.; Schiffrin, D. J. *J. Electroanal. Chem. Interfacial Electrochem.* **1984**, *179*, 277–284.
(67) Schiffrin, D. J.; Wiles, M. C.; Calder, M. R. *Extended Abstracts of The Electrochemical Society Spring Meeting*, Boston, May 4–9, 1986, pp 955–956.
(68) Yamane, M.; Kakiuchi, T.; Osakai, T.; Sanda, M. *Rev. Polarogr. (Kyoto)* **1983**, *29*, 102.
(69) Wandlowski, T.; Račinský, S.; Mareček, V.; Samec, Z. *J. Electroanal. Chem. Interfacial Electrochem.* **1987**, *227*, 281–285.
(70) Wandlowski, T.; Mareček, V.; Samec, Z. *J. Electroanal. Chem. Interfacial Electrochem.* **1988**, *242*, 277–290.
(71) Kakiuchi, T.; Kobayashi, M.; Senda, M. *Bull. Chem. Soc. Jpn.* **1987**, *60*, 3109–3115.
(72) Maeda, H.; Kakiuchi, T.; Senda, M. *Rev. Polarogr. (Kyoto)* **1987**, *33*, 38.
(73) Henderson, D.; Blum, L.; Lozada-Cassou, M. *J. Electroanal. Chem. Interfacial Electrochem.* **1983**, *150*, 291–303.
(74) Samec, Z.; Mareček, V.; Homolka, D. *J. Electroanal. Chem. Interfacial Electrochem.* **1983**, *158*, 25–36.
(75) Osakai, T.; Kakutani, T.; Senda, M. *Bull. Chem. Soc. Jpn.* **1985**, *58*, 2626–2633.
(76) Wandlowski, T.; Mareček, V.; Samec, Z. *J. Electroanal. Chem. Interfacial Electrochem.* **1988**, *242*, 391–402.
(77) Samec, Z.; Mareček, V.; Weber, J.; Homolka, D. *J. Electroanal. Chem. Interfacial Electrochem.* **1981**, *126*, 105–119.
(78) Samec, Z.; Homolka, D.; Mareček, V. *J. Electroanal. Chem. Interfacial Electrochem.* **1982**, *135*, 265–283.
(79) Kakutani, T.; Nishiwaki, Y.; Osakai, T.; Sanda, M. *Bull. Chem. Soc. Jpn.* **1986**, *59*, 781–788.
(80) Samec, Z.; Kharkats, Yu. I.; Gurevich, Yu. Ya. *J. Electroanal. Chem. Interfacial Electrochem.* **1986**, *204*, 257–266.